5.1 Introduction

The three different sized formulations of Darunavir loaded SLNs (Dar-SLN1, Dar-SLN2 and Dar-SLN3), peptide grafted Darunavir loaded SLNs (Pept-Dar-SLN), optimized Darunavir loaded nanoemulsion (DNE-3) and peptide grafted Atazanavir sulfate loaded SLNs (Pept-ATZ-SLN) were characterized for various parameters including particle size, zeta potential, microscopic analysis, differential scanning colorimetry (DSC) and Fourier transform-infrared spectroscopy (FT-IR) study.

In-vitro drug release studies are important in characterizing any kind of drug delivery system as it gives an insight about the *in-vivo* performance of that system as well as the parameters that helps to verify whether the delivery system developed is good enough for the expected purpose or any changes. For all the selected formulations, *in-vitro* drug release studies were performed in simulated gastric fluid and simulated intestinal fluid (SIF) as per US Pharmacopeia. In SIF, pancreatin was present which contains enzyme lipase that is expected to cause lipolysis of lipid. Hence, pancreatin was added. Sodium lauryl sulphate was added to maintain sink condition as well as to mimic fed conditions. Presence of food also influences *in-vitro* release. Triglycerides was produced which act as a surfactant and can increase bioavailability of Darunavir.

Kinetics of drug release: After performing drug release study, data were fitted in various models in order to examine the release mechanism of drug from the prepared formulations. Best fitting model was analyzed by regression coefficient method R^2 value. The following models were applied as described Costa et al. (1).

A. Zero order release

Following equation can be applied for drug release that follows zero order kinetics.

$$Q = K_0\, t$$

Where Q is the amount of drug release at time t and K_0 is the zero order release constant. Regression value of plot of amount of drug release versus time t gives the idea of release mechanism. R^2 value nearer to 1 indicates zero order release.

B. First order release

$$\ln(100 - Q) = \ln Q_0 - K_1 t$$

Where Q is the amount of drug release at time t and K_1 is the first order release constant. The regression coefficient (R^2) value obtained from the log % ARR (amount remaining to release) versus time, nearer to 1 indicates first order release.

C. Higuchi's model

$$Q = K_H t^{1/2}$$

Q is the amount of drug release at time t and K_H is the Higuchi square root of time release constant. The regression co-efficient of percentage drug release versus square root of time nearer to one indicates anomalous release (2, 3). This relation can be used to describe the drug dissolution from several types of modified release pharmaceutical dosage forms, as in the case of some transdermal systems and matrix tablets with water soluble drugs.

D. Korsmeyer - Peppas model

$$Log\left(\frac{M_t}{M_\alpha}\right) = Log\ K + n Log\ t$$

Where Mα is the total drug release after infinite time, Mt/Mα is the fractional of drug release at time t, K is the kinetic constant incorporating structural and geometrical characteristic of the drug/polymer system (devices), n is the diffusion exponents that characterizes the mechanism of drug release and t is the time. Graph of log % drug release versus log time is plotted, n value is obtained and release kinetic is determined using following specifications. This type of drug release is controlled by combination of polymer swelling, erosion and diffusion through the hydrated matrix (Diffusion and chain relaxation).

The value of n<0.5 or n=0.5 indicating fickian diffusion

The value of n between 0.5 to 1 (0.5 < n <1) indicating non-fickian release

The value of n = 1, indicating the Zero order release or case 2 transport

The value of n >1, indicating the Super case 2 transport

This model is generally used to analyze the release of pharmaceutical polymeric dosage forms, when the release mechanism is not well known or when more than one type of release phenomena could be involved (4, 5).

E. Hixon Crowell model

Following equation can be applied for drug release that follows Hixon Crowell kinetics model.

$$3\sqrt{Q_0} - 3\sqrt{Q_t} = K_H t$$

A plot of $3\sqrt{Q_0} - 3\sqrt{Q_t}$ Versus t is plotted where Q0 is the initial concentration of drug present, Qt is the amount of drug release at time t and KH is the kinetic constant for distribution from constantly changing surface area observed in slow dissolving tablets (6).

5.2 Materials

Pepsin (800-2500 units per mg protein) and pancreatin were purchased from Himedia, Mumbai. Sodium sulphide, sulphuric acid, glycerine, sodium chloride, hydrochloric acid, sodium lauryl sulphate, monobasic potassium phosphate, sodium dihydrogen phosphate, disodium hydrogen phosphate, sodium bicarbonate, sodium hydroxide and dithiothreitol (DTT) were purchased from S.D.Fine chem Ltd. (Mumbai, India). Methanol and acetic acid were purchased from spectrochem (Mumbai, India). N,N,N',N'- tetramethylethylenediamine (TEMED), Acrylamide, bis-acrylamide, Tris (hydroxymethyl) aminomethane (Trisbase) and bovine serum albumin were obtained from Himedia Lab. (Mumbai, India). Ammonium persulfate was purchased from Sigma-aldrich. Distilled water was prepared in laboratory.

5.3 Characterization of optimized Darunavir loaded solid lipid nanoparticles formulations

5.3.1 Particle size and zeta potential

The particle size and zeta potential of optimized nanoparticle formulations (Dar-SLN1, Dar-SLN2 and Dar-SLN3) were determined using Malvern zetasizer (Nano ZS, malvern instrument, UK). The samples were diluted 10 times with filtered distilled water to avoid multi-scattering phenomena and placed in disposable sizing cuvette. Zeta potential calculation was performed by zetasizer software using smoluchowski's equation from the electrophoretic mobility. Each determination for size and zeta potential was repeated in triplicate and the results were expressed as mean value ± SD (standard deviation).

5.3.2 Entrapment efficiency (EE) and drug loading

The nanoparticle formulations were filled in cellulose dialysis bag (MWCO 12000 Da, Sigma, Germany) and dialyzed with magnetic stirring (50 rpm; Remi, Mumbai, India) against double distilled water under sink conditions for 10 min to remove any unentrapped drug from the formulation (7). After dialysis, the nanoparticles were dissolved using methanol: dichloromethane (7:3) solvent mixture, diluted suitably and analyzed by developed UV method (chapter 3). EE and drug loading were calculated using following formulae:

$$\%\ EE = \frac{amount\ of\ entrapped\ drug}{total\ amount\ of\ drug\ added}\ x\ 100$$

$$\%\ drug\ loading = \frac{amount\ of\ entrapped\ drug}{total\ weight\ of\ nanoparticles}\ x100$$

5.3.3 Transmission electron microscopy (TEM) and Field emission scanning electron microscopy (FE-SEM)

The nanoparticle suspensions were negatively stained and the grid of samples prepared thereof were examined under transmission electron microscope (Hitachi H-7500, 120 kV) and the images were captured. The study was performed for all three optimized formulations. The morphology of optimized nanoparticles formulations after lyophilization was examined using scanning electron microscopy study. The samples were coated with platinum (3mm thick) using an Ion sputter for 5 min at 20 mA. Observation was performed at an accelerating voltage for 60 kV and a working distance of 7.7 mm. The images were recorded using field emission scanning electron microscope (JEOL, JSM7600F).

5.3.4 Differential scanning calorimetric (DSC) studies

DSC studies were performed for pure drug, HCO, physical mixtures of drug: lipid (1:0.5, 1:1, and 1:6), placebo solid lipid nanoparticles and lyophilized form of Dar-SLN2 in order to characterize the physical state of drug in nanoparticles. All samples were dried in desiccators for 24 hr before the thermal analysis. Small amount of samples were sealed

in standard aluminium pans with lids and heated at a rate of 2ºC/min from 20-300ºC. Dry nitrogen gas was passed through DSC cell at a flow rate of 40 ml/min. The thermograms were obtained using DSC-60 (schimadzu, Japan).

5.3.5 Fourier transform infrared (FT-IR) spectroscopy

FT-IR study was performed to detect the possibilities of interaction between Darunavir and excipients used in the formulation. The samples analyzed were pure drug, HCO, physical mixture of drug and lipid (1:6) and lyophilized formulation Dar-SLN2. The samples were dried in desiccators for 24 hr before the analysis. The samples were mixed with KBr, placed in sample holder and analyzed using Fourier transform infrared spectrophotometer (IRAffinity-1, Shimadzu).

5.3.6 *In-vitro* drug release study

5.3.6.1 Activation of dialysis membrane

Before using the dialysis membrane for drug release study it was first activated by following procedure (8).

1. 5 cm long dialysis membrane was cut and was kept in running water for 3 hr for the removal of glycerine.
2. Dialysis membrane was then dipped in 0.3% w/v solution of Sodium sulphide solution at 80ºC for 1min.
3. Sodium sulphide treated Dialysis membrane was then dipped in warm water at 60ºC for 1 min to remove sodium sulphide.
4. Dialysis membrane was then dipped in 0.2 % H_2SO_4 for 1 min.
5. Then it was again dipped in the warm water for removal of H_2SO_4.

This activated dialysis membrane was then kept in Phosphate buffer saline (pH 7.4) for 24 hr prior to drug release studies.

5.3.6.2 Preparation of solutions (9)

Simulated gastric fluid, pH 1.2 with 0.5 % w/v SLS: 2 g sodium chloride and 3.2 g pepsin were accurately weighed and dissolved in 500 ml distilled water. 7 ml

hydrochloric acid and 5 g sodium lauryl sulphate (SLS) was added to it. Final volume was made up to 1000 ml with distilled water.

Simulated intestinal fluid, pH 7.4 with 0.5 % w/v SLS: 6.8 g monobasic potassium phosphate was dissolved in 250 ml distilled water. 77 ml 0.2 N sodium hydroxide was added to 500 ml distilled water. Both these solutions were mixed and 10 g pancreatin as well as 5 g sodium lauryl sulphate was added in to it. pH was adjusted to 6.8 with 0.2 N NaOH or 0.2 N HCl. The final volume was made up to 1000 ml.

5.3.6.3 Protocol

The *in-vitro* release studies for Dar-SLN1, Dar-SLN2 and Dar-SLN3 were performed as described by Neves et al. (10). Briefly, SLN dispersion containing 20 mg drug was taken in activated dialysis membrane (MWCO- 12000, Hi media, India) closed as one end. The other end was closed and suspended in beaker containing 50 ml SGF for 2 hr followed by 50 ml SIF for 12 hr. The beaker was maintained at constant stirring at 100 rpm using magnetic stirrer at 37 ^{o}C ± 0.5^{o}C throughout the experiment. At predetermined time intervals, 2 ml samples were withdrawn from the receptor compartment (media) and sink conditions were maintained by addition of fresh media. The withdrawn samples were diluted appropriately and analyzed by UV spectroscopy at the absorbance maxima of 267 nm as per developed method (section 3.3.3 and 3.3.4). The cumulative percentage of released drug was determined using the average of the triplicate experiments. The release of drug from Darunavir suspension (as control) was also studied similarly. After performing drug release study, data were fixed in various models and best fitting model was analyzed by correlation coefficient (R^2) method. R^2 value nearer to 1 indicates best suitable release mechanism.

5.4 Characterization of peptide attached solid lipid nanoparticles of Darunavir

5.4.1 Particle size and zeta potential

The particle size and zeta potential of Darunavir loaded SLNs after attachment of peptide was determined by procedure mentioned in section 5.3.1. Each determination for size and zeta potential was performed in triplicate and the results are expressed as mean value ± SD.

5.4.2 Qualitative determination of surface grafted peptide (11, 12)

Principle: SDS-PAGE uses an anionic detergent (SDS) along with reducing agent mercaptoethanol (which reduce all disulfide bonds) to denature proteins. One SDS molecule binds to 2 amino acids. Due to this, the charge to mass ratio of all the denatured proteins in the mixture becomes constant. These protein molecules move in the gel (towards the anode) on the basis of their molecular weights and are separated.

Preparation of reagents:

30 % Acrylamide: It was prepared by dissolving 29.2 gm acrylamide and 0.8 gm bis-acrylamide in 100 ml distilled water.

10% SDS: 10g SDS was weighed accurately and dissolved in 100 ml distilled water.

10% Ammonium persulfate: 1 g Ammonium persulfate was dissolved in water and volume was made up to 10 ml using distilled water.

Tris-glycine buffer (Running Buffer- 5X stock solution): 15.1 gm Tris base, 94 gm glycine, 50 ml 10 % SDS were added in distilled water and volume was made up to 1 L using distilled water.

Tris-Cl buffer 1.0 M, pH=6.8: 12.114 gm Tris base was dissolved in 70 ml distilled water. The pH was adjusted to 6.8 using HCl and the final volume was made up to 100 ml with distilled water.

Tris-Cl buffer 1.5 M, pH=8.8: 18.17 gm Tris base was dissolved in 70 ml distilled water. The pH was adjusted to 8.8 using HCl and the final volume was made up to 100 ml with distilled water.

5 % Stacking gel: The components of stacking gel are given below:

Table 5.1 Composition of 10 ml of stacking gel

Components	Volume in ml of components for making 10 ml gel
Distilled water	6.8

30 % acrylamide	1.7
Tris-Cl (1.0 M, pH=6.8)	1.25
10 % SDS	0.1
10 % Ammonium persulfate	0.1
TEMED	0.01

15 % resolving gel: The components of resolving gel are given below:

Table 5.2 Composition of 10 ml of resolving gel

Components	**Volume in ml of components for making 10 ml gel**
Distilled water	2.3 ml
30 % acylamide	5 ml
Tris-Cl (1.5 M, pH=8.8)	2.5 ml
10 % SDS	0.1 ml
10 % Ammonium persulfate	0.1 ml
TEMED	4 µL

Staining reagent: The staining reagent consisted of 40 % Methanol, 10 % Acetic acid and 0.1 % Coomassie Blue R-250 in distilled water.

Destaining reagent: It consisted of 20 % methanol and 10 % glacial acetic acid in distilled water.

Procedure:

i. Casting of gels
   - The glass plates and apparatus were assembled as per manufacturer's instructions.
   - Stacking gel and resolving gel were prepared as per procedure mentioned above.
   - The resolving gel monomer solution was prepared by combining all reagents (Table 5.2) except ammonium persulfate (APS) and TEMED.

- The comb was placed completely into the assembled gel sandwich and with a marker pen, a mark was done on the glass plate 1 cm below the teeth of the comb which indicated the level to which the resolving gel was to be poured.
- The comb was removed.
- APS and TEMED were added to the monomer solution, mixed well and the resulting solution was poured up to the mark.
- The monomer solution was overlaid immediately with 1 ml of isobutanol.
- The gel was allowed to polymerize for 45 minutes to 1 hour. After that isobutanol was poured off.
- The stacking gel monomer solution was prepared.
- Comb was placed in the gel sandwich.
- APS and TEMED were added to the solution and the solution was poured down through one of the spacer until the sandwich was completely filled.
- The gel was allowed to polymerize for 15 minutes.
- The comb was removed.
- Gel was placed in the buffer chamber and running gel buffer was added into the chamber.

ii. Preparation of samples

Four samples were prepared: (a) sample 1: Peptide solution in non reducing condition (not containing DTT), (b) sample 2: Peptide solution in reducing condition (contains DTT), (c) sample 3: Formulation in non reducing condition and (d) sample 4: Formulation in reduced condition. Following components were taken in eppendorfs for each sample:

Peptide stock/ Formulation- (standard- 10µg final loading)

Dithiothreitol (DTT) – 0.15 M (For reducing condition only)

SDS- 4 %

Glycerol – 10 %

Bromophenol blue – (0.01 %)

iii. Loading of gels

The samples were carefully loaded in the wells using 10 µl micropipette.

iv. Running the gel

- The buffer was filled in the upper buffer chamber fully as there might be chances of leakage.
- The electrodes were connected both to electrolysis chamber and power supply unit.
- The gel was run at a constant voltage of 100 V.
- The electrophoresis was stopped when the tracker dye was ~ 1 cm above the end of the glass plates.

v. Removing and staining the gels

- The gel was removed from the buffer chamber and the glass plate sandwich was removed from it.
- Two plates were separated carefully and the gel was scraped from the plate.
- The gel was then placed in the container containing the Coomassie blue stain such that the gel was fully submerged in the staining solution. The gel was stained for 2 hrs.
- The gel was destained using a destaining solution until protein bands were visualized.
- The bands were observed using Gel-Doc instrument (Genaxy, India).

5.4.3 Quantitative determination of bound peptide

The quantitative determination of bound peptide was done by Lowry's method (13).

Principle:

- Reactivity of the peptide nitrogen[s] with the copper [II] ions under alkaline conditions and the subsequent reduction of the Folin-Ciocalteay phosphomolybdic phosphotungstic acid to heteropolymolybdenum blue by the copper catalyzed oxidation of aromatic acids.
- The phenolic group of tyrosine and tryptophan residues (amino acid) in a protein will produce a blue purple color complex, with maximum absorption in the region of 660

nm wavelength, with Folin- Ciocalteu reagent. Thus the intensity of color depends on the amount of these amino acids present and will thus vary for different proteins.

- Most proteins estimation techniques use Bovin Serum Albumin (BSA) universally as a standard protein, because of its low cost, high purity and ready availability.

Solutions prepared:

Solution A (500 ml): 2.8598 gm NaOH, 14.3084 gm Na_2CO_3

Solution B (100 ml): 1.4232 gm $CuSO_4.5H_2O$,

Solution C (100 ml): 2.85299 gm Sodium potassium tartrate

Lowry solution: Solution A + Solution B + Solution C in ratio of 100:1:1

Folin reagent: 1 ml Folin-Ciocalteu's reagent + 1 ml distilled water

Procedure:

0.5 ml of the sample was taken in the 2 ml eppendorff tube (For formulation sample, 0.25ml of Pept-Dar-SLN was diluted to 0.5 ml with buffer (0.9% NaCl, 10mM $NaHCO_3$) and taken for study). 0.7 ml of Lowry solution was added, vortexed and incubated in dark at room temperature for 15 min. After incubation, 0.1 ml of diluted Folin reagent was added, vortexed and again incubated in dark for 30 min. After 30 min the samples were analyzed colorimetrically at 660 nm wavelength using UV-Vis spectrophotometer. The calibration curve was prepared using BSA as standard and concentration of peptide in sample was calculated from its absorbance and calibration equation. % conjugation- % of peptide conjugated to nanoparticles was calculated from the following equation:

$$\%\ conjugation = \frac{Amount\ of\ peptide\ conjugated}{Theoretical\ amount\ of\ peptide\ in\ sample}\ X\ 100$$

5.4.4 *In-vitro* drug release study

The *in-vitro* release studies for Pept-Dar-SLN was performed as per procedure mentioned in section 5.3.6.

5.5 Characterization of nanoemulsion of Darunavir

5.5.1 Globule size, PDI and Zeta potential

Globule size, PDI and zeta potential of nanoemulsion was measured by Malvern Zetasizer after proper dilution.

5.5.2 Electrical conductivity

The electrical conductivity of DNE-3 was determined using conductivity meter (306, Systronics, India). The measurement was performed by direct immersion of electrode into the sample.

5.5.3 Drug loading

For estimation of drug loading, an aliquot of formulation was dissolved in methanol: dichloromethane (7:3) and analyzed by UV spectrophotometry using developed calibration plot (chapter 3). The % drug loading was calculated using following formula.

$$Drug\ loading = \frac{amount\ of\ entrapped\ drug}{total\ volume\ of\ nanoemulsion\ formulation}$$

5.5.4 Transmission electron microscopy

The optimized formulation DNE-3 was negatively stained and the grid of sample prepared thereof was examined under transmission electron microscope (Hitachi H-7500, 120 kV) and the image was captured.

5.5.5 *In-vitro* drug release study

The *in-vitro* release studies for DNE3 was performed by dialysis bag technique. Briefly, nanoemulsion containing 20 mg drug was taken for the study and procedure was followed as mentioned in section 5.3.6. The study was conducted for 12 hr (2 hr in SGF and rest in SIF). The results were compared with the drug release from Darunavir suspension (control) prepared using 0.4% w/v methyl cellulose and the kinetics of drug

release mechanism was studied. Darunavir suspension was prepared using 0.4 % w/v methyl cellulose.

5.6 Characterization of optimized ATZ loaded solid lipid nanoparticles (ALN-23) and peptide grafted ATZ loaded SLNs (Pept-ATZ-SLN)

5.6.1 Particle size and zeta potential

The particle size and zeta potential of ALN-23 and Pept-Dar-SLN were determined using Malvern zetasizer (Nano ZS, malvern instrument, UK) as per procedure mentioned in section 5.3.1. The measurements for size and zeta potential were performed in triplicate and the results were expressed as mean value ± SD.

5.6.2 EE and drug loading

The nanoparticle formulations were filled in cellulose dialysis bag (MWCO 12000 Da, Sigma, Germany) and dialyzed with magnetic stirring (50 rpm; Remi, Mumbai, India) against double distilled water under sink conditions for 10 min to remove any unentrapped drug from the formulation (7). After dialysis, the nanoparticles were dissolved using methanol: dichloromethane (7:3) solvent mixture, diluted suitably and analyzed by developed UV method (chapter 3). EE and drug loading were estimated using following formulae:

$$\%\ EE = \frac{amount\ of\ entrapped\ drug}{total\ amount\ of\ drug\ added}\ x\ 100$$

$$\%\ drug\ loading = \frac{amount\ of\ entrapped\ drug}{total\ weight\ of\ nanoparticles}\ \text{x}\ 100$$

5.6.3 TEM and FE-SEM

The nanoparticle suspension of ALN-23 optimized formulation was negatively stained and the grid of sample prepared thereof was examined under transmission electron microscope (Hitachi H-7500, 120 kV) and the image was captured. The morphology of optimized nanoparticles formulation ALN-23 after lyophilization was examined using scanning electron microscopy study. The sample was coated with

platinum (3mm thick) using an Ion sputter for 5 min at 20 mA. Observation was performed at an accelerating voltage for 60 kV and a working distance of 7.7 mm. The image was recorded using field emission scanning electron microscope (JEOL, JSM7600F).

5.6.4 DSC studies

DSC studies were performed for pure ATZ, HCO, physical mixtures of drug and lipid and lyophilized form of ATZ loaded nanoparticles (ALN-23) in order to characterize the physical state of drug in nanoparticles. All samples were dried in desiccators for 24 hr before the thermal analysis. Small amount of samples were sealed in standard aluminium pans with lids and heated at a rate of 2ºC/min from 20-300ºC. Dry nitrogen gas was passed through DSC cell at a flow rate of 40 ml/min. The thermograms were obtained using DSC-60 (schimadzu, Japan).

5.6.5 FT-IR spectroscopy

FT-IR study was performed to detect the possibilities of interaction between ATZ and excipients in the formulation. The samples analyzed were pure drug, HCO, physical mixture of drug and lipid and lyophilized formulation ALN-23. The samples were dried in desiccators for 24 hr before the analysis. The samples were mixed with KBr, placed in sample holder, compressed into pellet and analyzed using Fourier transform infrared spectrophotometer (IRAffinity-1, Shimadzu).

5.6.6 Qualitative and quantitative determination of surface grafted peptide

The amount of peptide bound to nanoparticles was determined qualitatively and quantitatively as per procedure mentioned in sections 5.3.2 and 5.3.3.

5.6.7 *In-vitro* drug release of Atazanavir loaded solid lipid nanoparticles

The *in-vitro* release studies were conducted for lyophilized samples of optimized ATZ loaded SLNs (ALN-23) and peptide attached SLNs of ATZ (Pept-ATZ-SLN) by dialysis bag technique. Briefly, nanoparticles containing 40 mg drug was taken for the

study and other procedure was followed as mentioned in section 5.3.6. The study was conducted for 12 hr (2 hr in SGF and rest in SIF). The samples were analyzed by UV spectroscopy at the absorbance maxima of 249 nm as per developed method (section 3.4.3 and 3.4.4). The cumulative percentage of released drug was determined using the average of the triplicate samples. The release of drug from ATZ suspension (prepared using 0.4 % w/v methyl cellulose) as control was also studied similarly for comparison.

5.7 Results and discussion

5.7.1 Characterization of optimized Darunavir loaded SLN formulations

5.7.1.1 Particle size and zeta potential

Figure 5.1, Figure 5.2 and Figure 5.3 shows the particle size distribution of Dar-SLN1, Dar-SLN2 and Dar-SLN3 respectively. The mean particle sizes for all three formulations were found to be 93.28 ± 3.62 nm, 189.45 ± 2.10 and 527.62 ± 2.15 along with PDI of 0.191 ± 0.01, 0.115 ± 0.024 and 0.114 ± 0.031 respectively. PDI measures the relative variance in the particle size distribution. In general, higher the PDI, the lower the uniformity of the particle size (14). The low PDI vales obtained here indicates the more uniformity in the particle size. The zeta potential analysis of formulations- Dar-SLN1, Dar-SLN2 and Dar-SLN3 is shown in Figure 5.4, Figure 5.5 and Figure 5.6 respectively. The values obtained were -48.82 ± 2.14, -50.1 ± 1.17 and -49.23 ± 2.28 mV for Dar-SLN1, Dar-SLN2 and Dar-SLN3 respectively. Negative zeta values might be due to HCO. There was no significant difference in zeta potential of all three formulations. Generally, zeta potential values > 30mV and < -30mV are considered as high values and leads to colloidal stability due to repulsion between them (15). The formulated SLNs showed high zeta values thus a good colloidal stability can be expected.

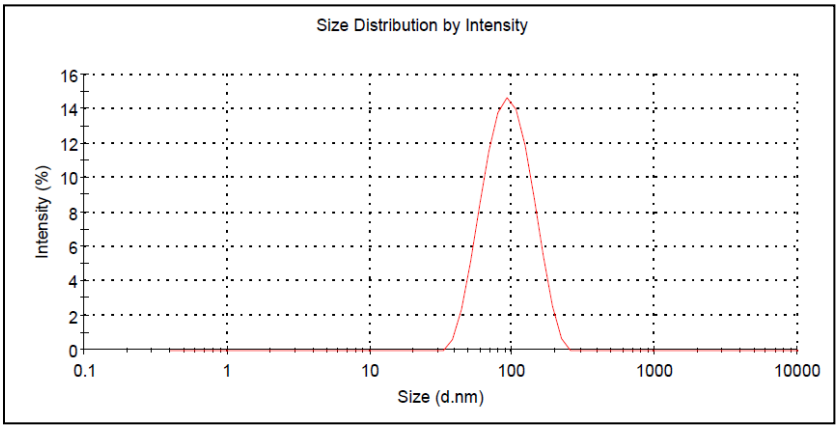

Figure 5.1 Particle size distribution of Dar-SLN1 formulation

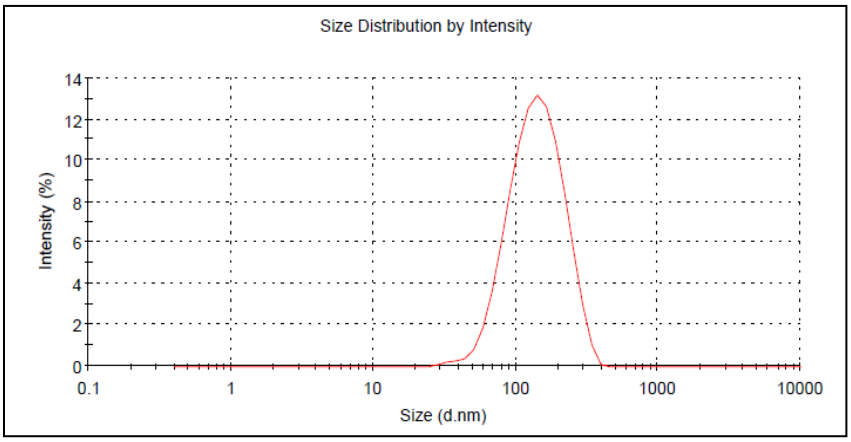

Figure 5.2 Particle size distribution of Dar-SLN2 formulation

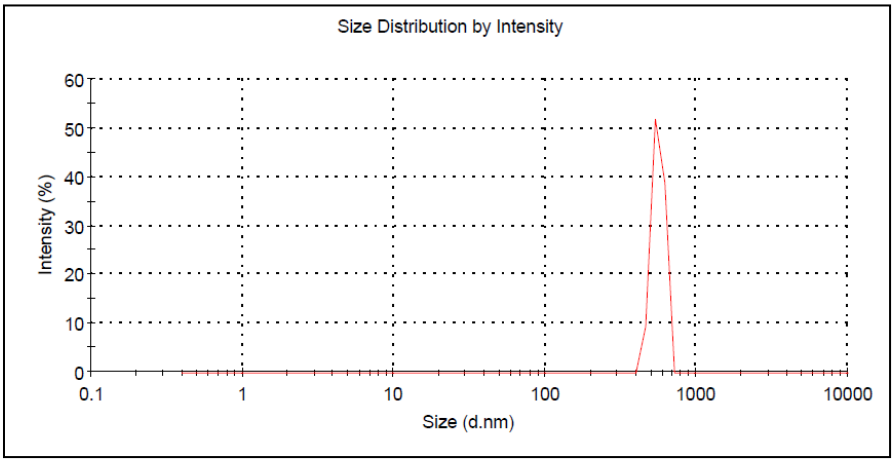

Figure 5.3 Particle size distribution of Dar-SLN3 formulation

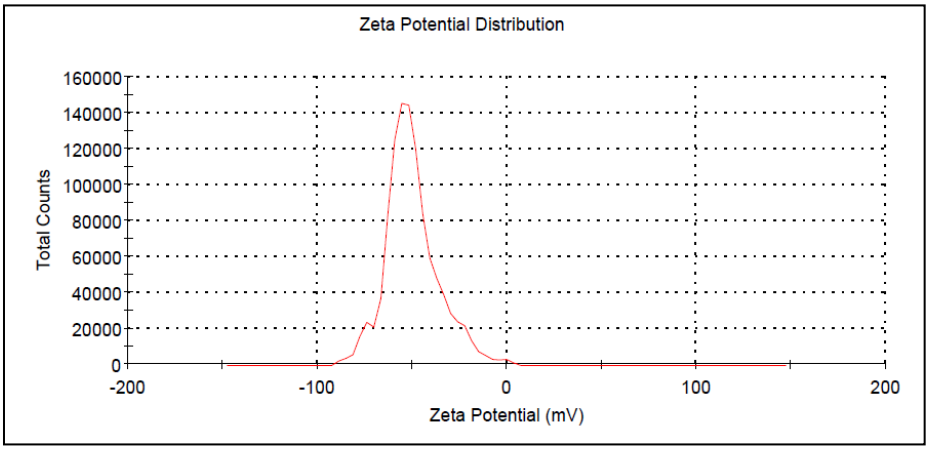

Figure 5.4 Zeta potential of Dar-SLN1 formulation by Malvern Zetasizer

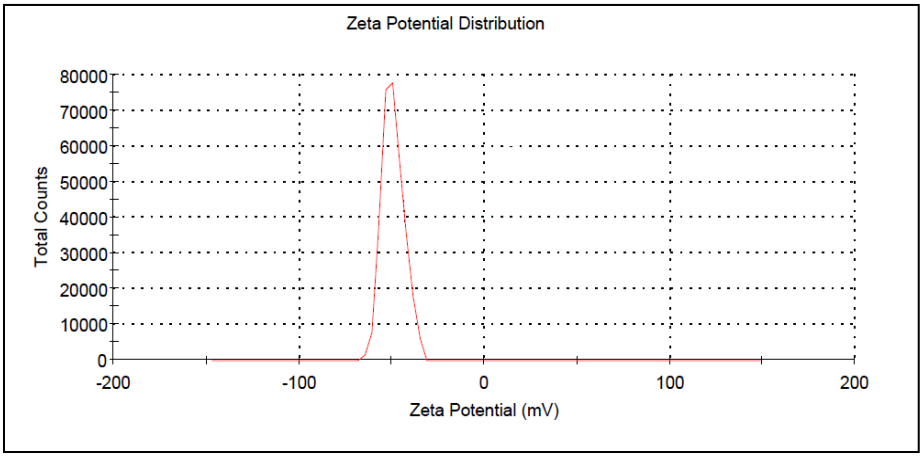

Figure 5.5 Zeta potential of Dar-SLN2 formulation by Malvern Zetasizer

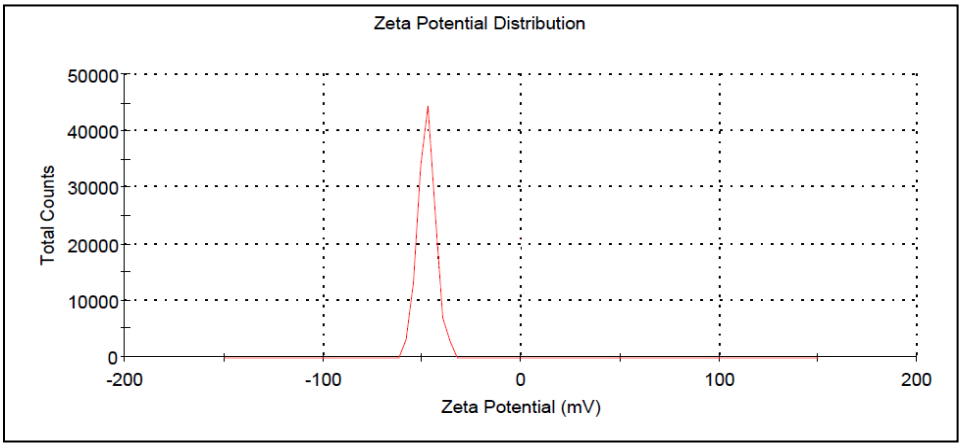

Figure 5.6 Zeta potential of Dar-SLN3 formulation by Malvern Zetasizer

5.7.1.2 EE and drug loading

The values of % EE for Dar-SLN1, Dar-SLN2 and Dar-SLN3 formulations were found to be 89.09 ± 2.4, 90.10 ± 1.15 and 88.13 ± 2.26 % respectively and their drug loading were estimated as 12.92 ± 2.12, 13.06 ± 1.18 and 12.87 ± 1.67 % w/w respectively. The high entrapment efficiency obtained is attributed to the lipophilic drug having high affinity for the lipid. The insignificant difference in the entrapment of the three formulations is due to the similar formulation parameters.

5.7.1.3 TEM and FE-SEM

Figure 5.7, Figure 5.8 and Figure 5.9 shows transmission electron microscopic images of Dar-SLN1, Dar-SLN2 and Dar-SLN3 respectively while their FE-SEM images are shown in Figure 5.10, Figure 5.11and Figure 5.12 respectively. The images revealed the discrete and round structures without aggregation. The diameter of all three nanoparticles formulations were in accordance with the results obtained through size analysis (Malvern zetasizer). A large negative zeta potential obtained was advantageous for achieving lower particles, owing to the particles remaining discrete without agglomeration (as seen in TEM image) (16). Agglomeration may lead to increase in the size and losing its characteristics of enhanced absorption and lymphatic targeting.

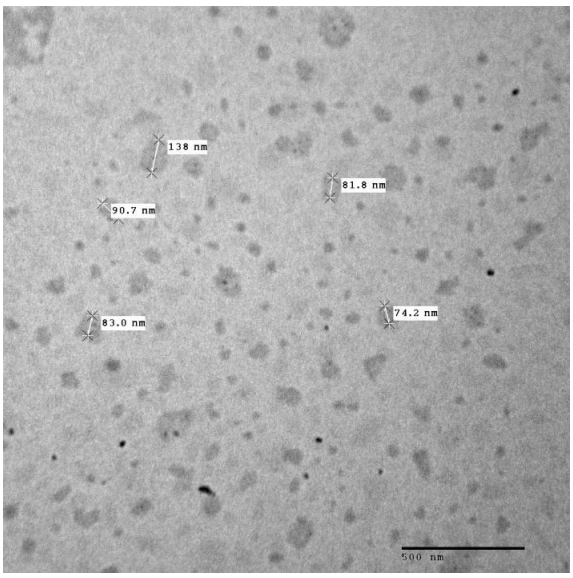

Figure 5.7 Transmission electron microscopic image of Dar-SLN1 formulation

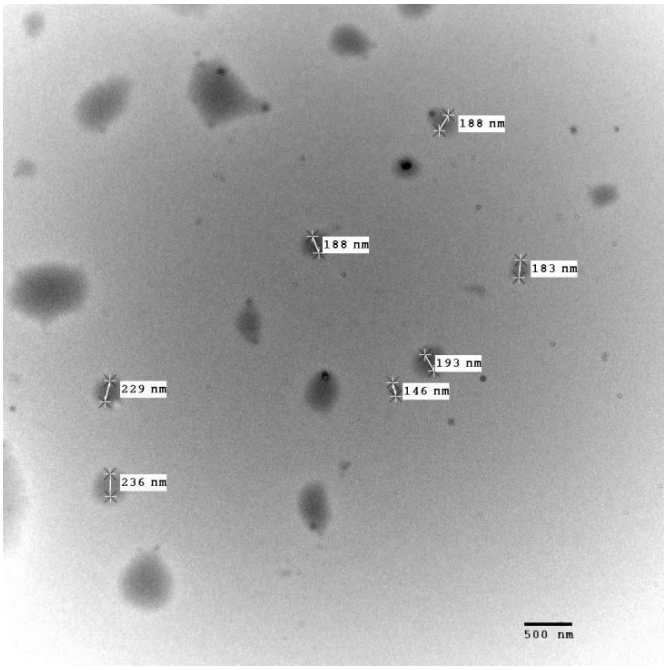

Figure 5.8 Transmission electron microscopic image of Dar-SLN2 formulation

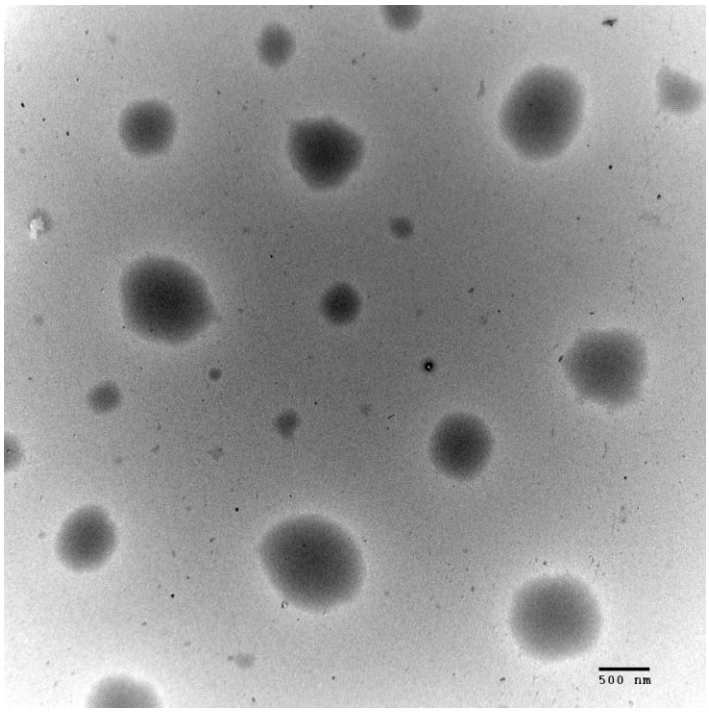

Figure 5.9 Transmission electron microscopic image of Dar-SLN3 formulation

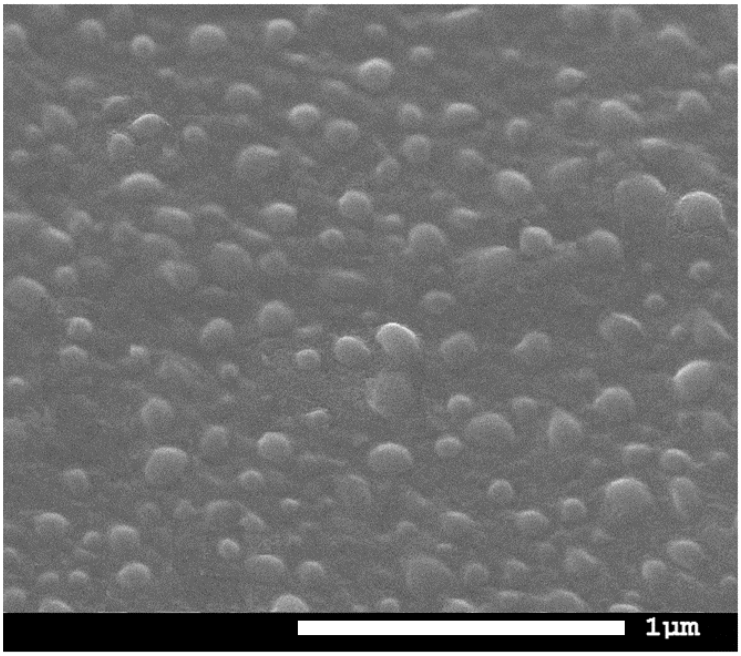

Figure 5.10 Field emission scanning electron microscopic image of Dar-SLN1 formulation

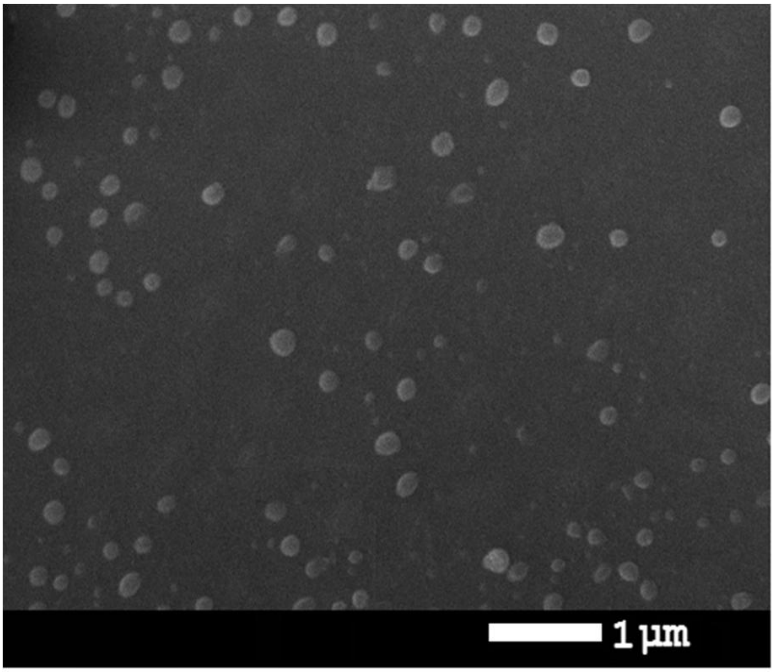

Figure 5.11 Field emission scanning electron microscopic image of Dar-SLN2 formulation

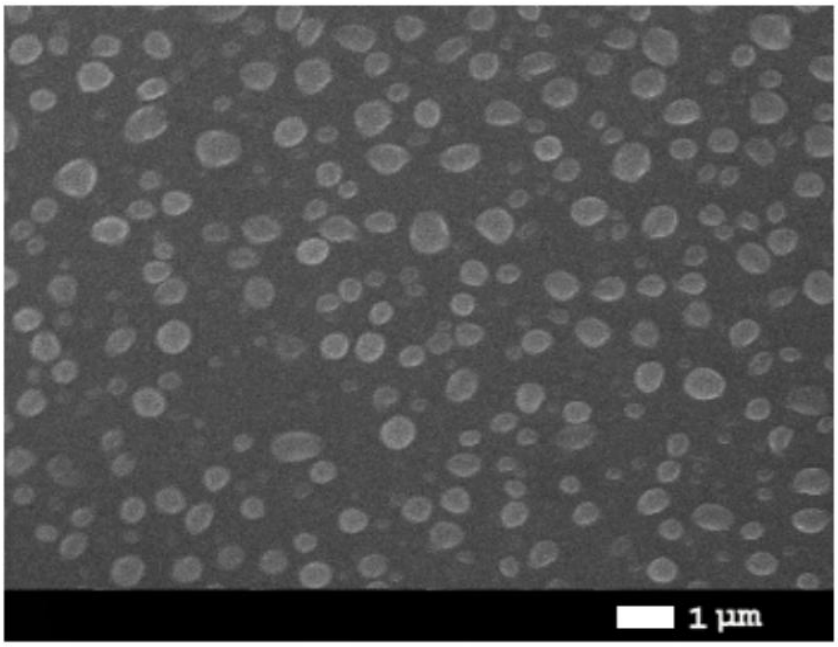

Figure 5.12 Field emission scanning electron microscopic image of Dar-SLN3 formulation

5.7.1.4 DSC studies

For assessment of miscibility of drug in lipid matrices, DSC study was done. The DSC thermogram of pure drug showed a sharp endothermic peak at 71.58ºC corresponding to its melting point (Figure 5.13). DSC thermogram of lipid showed two endothermic peaks at 76.51ºC and 85.19ºC due to its two isoforms (17). The DSC thermograms of physical mixtures in increasing ratio of drug: lipid (1:0.5, 1:1 and 1:6) were recorded. At ratio 1:0.5, three peaks were observed indicating one peak of drug and other two peaks of lipid. The peaks of drug and a peak of lipid were found to merge upon increasing drug: lipid ratio. Finally at ratio 1:6, there were only two peaks at 75.21ºC and 84.06ºC indicating the merging of drug peak with one peak of lipid. Similar results were observed with drug unloaded and drug loaded SLN formulation Dar-SLN2 (Figure 5.14). The DSC thermogram of both formulations were similar and absence of drug peak in drug loaded formulation indicates the homogenous distribution of drug in the lipid matrix (18).

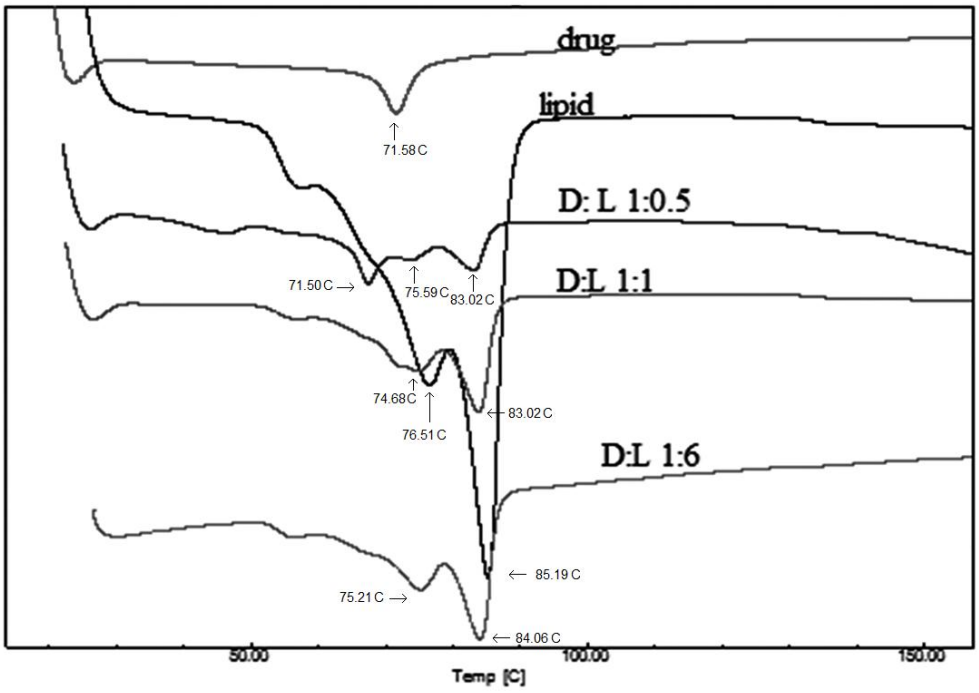

Figure 5.13 Overlay plot of DSC thermograms of pure drug, lipid and physical mixtures of drug and lipid in various ratios

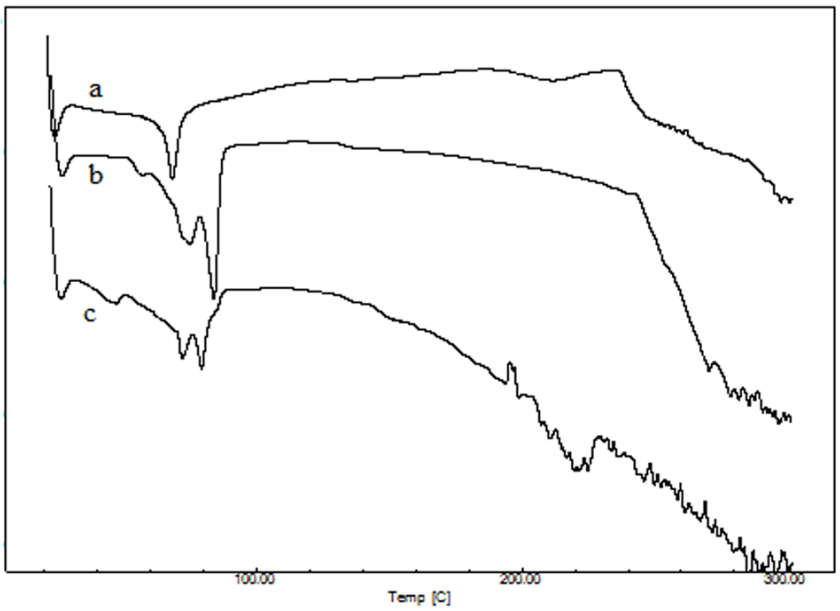

Figure 5.14 Overlay plot of DSC thermograms of (a) pure drug, (b) placebo solid lipid nanoparticles and (c) Darunavir loaded solid lipid nanoparticles (Dar-SLN2)

5.7.1.5 FT-IR spectroscopy

FT-IR spectrum of pure drug (Figure 5.15) showed characteristic peaks of N–H bending at 1593.20 cm^{-1}, CO stretching at 1249.87 cm^{-1}, C-N stretching at 1180.52 cm^{-1}, C-O-C stretching at 1145.01 cm^{-1} and aryl thio stretching at 700.16 cm^{-1} (19, 20). The spectrum of HCO (Figure 5.16) showed characteristics peaks of –C=O stretching at 1737.86 cm^{-1}, methylene $(CH_2)_n$ rocking at 719.45 cm^{-1} and CH_2 stretching at 2914.44 and 2846.33 cm^{-1}. These peaks of lipid were found to be retained upon nanoparticle formulation as seen in spectrum of placebo solid lipid nanoparticles (

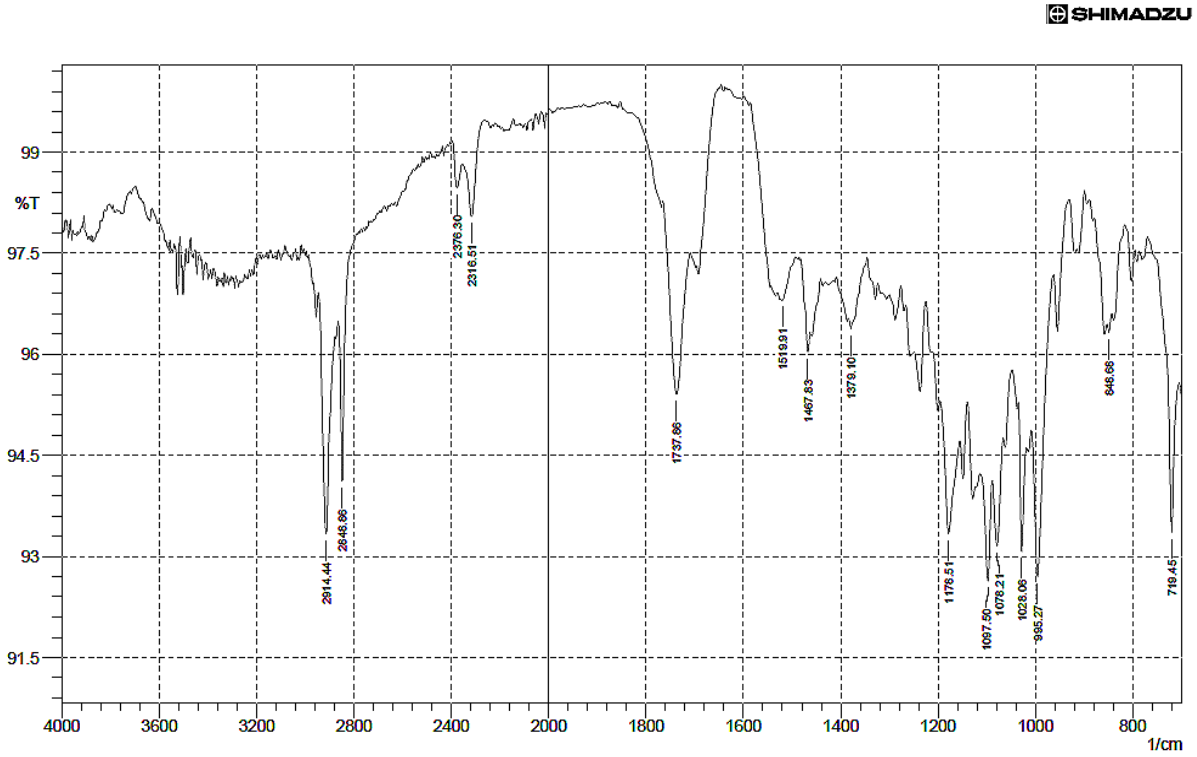

Figure **5.18**). The interpretation of peaks found in all the spectra is given in Table 5.3 and Table 5.4. The spectrum of physical mixture (Figure 5.17) and lyophilized formulation (Figure 5.19) showed characteristic peaks of both drug and lipid indicating compatibility of drug with excipients of the formulation.

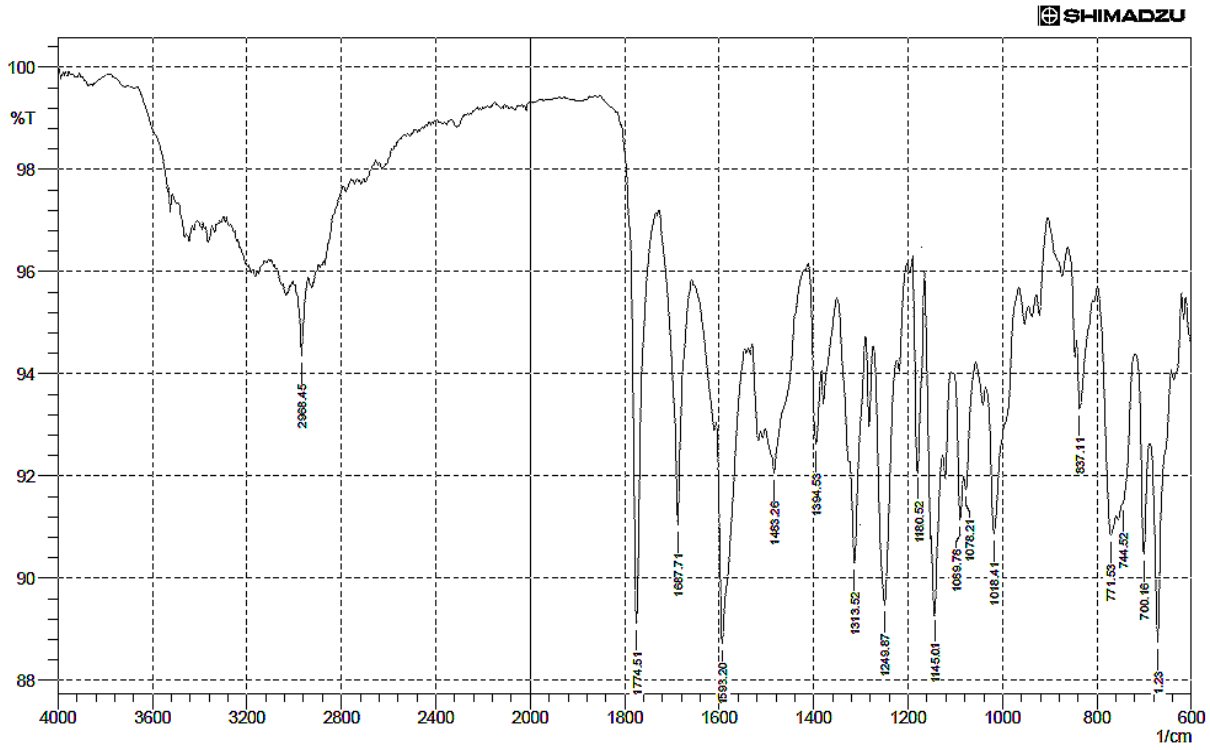

Figure 5.15 FT-IR spectrum of Darunavir

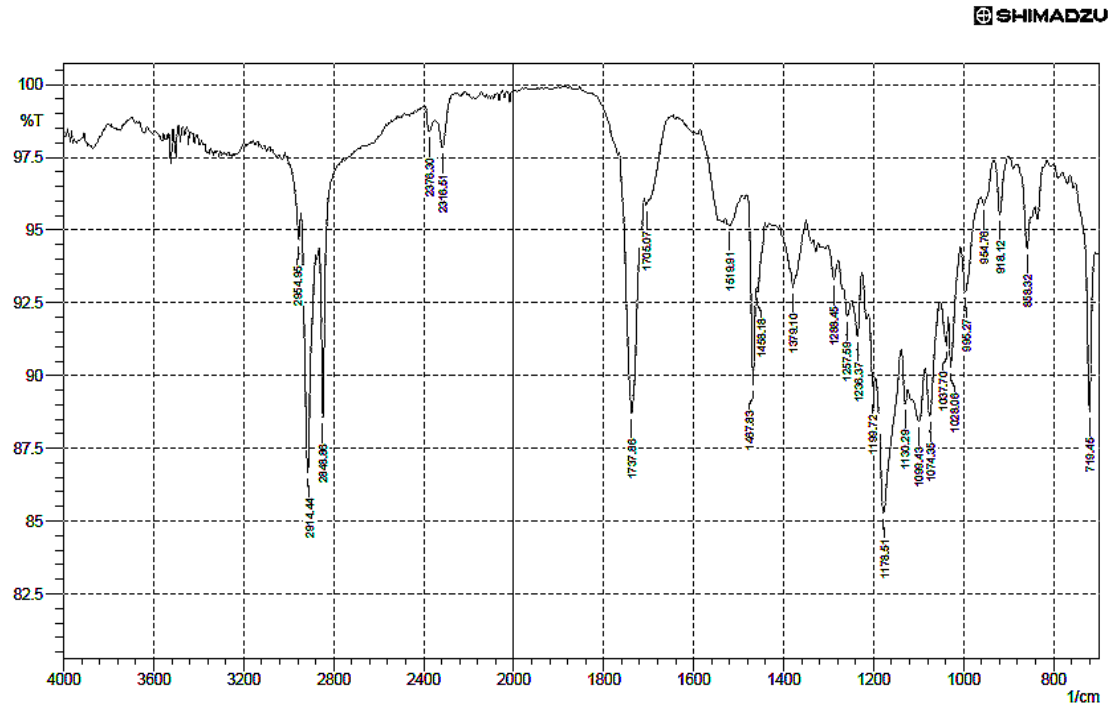

Figure 5.16 FT-IR spectrum of hydrogenated castor oil

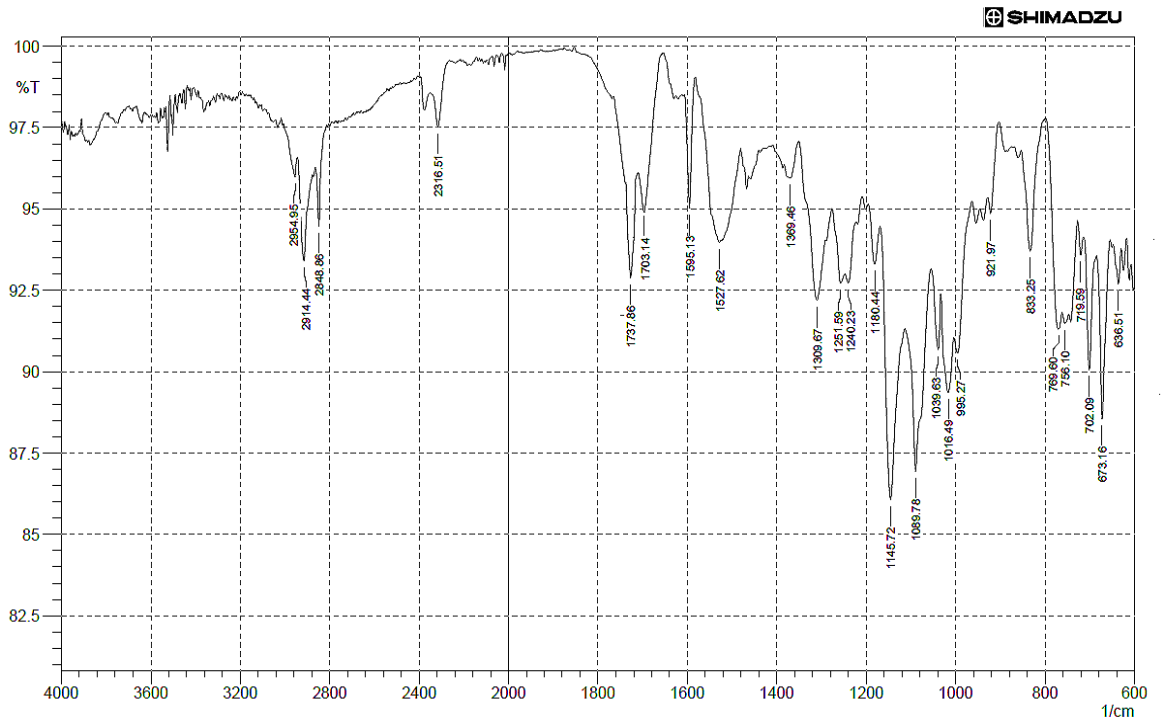

Figure 5.17 FT-IR spectrum of physical mixture of drug and HCO

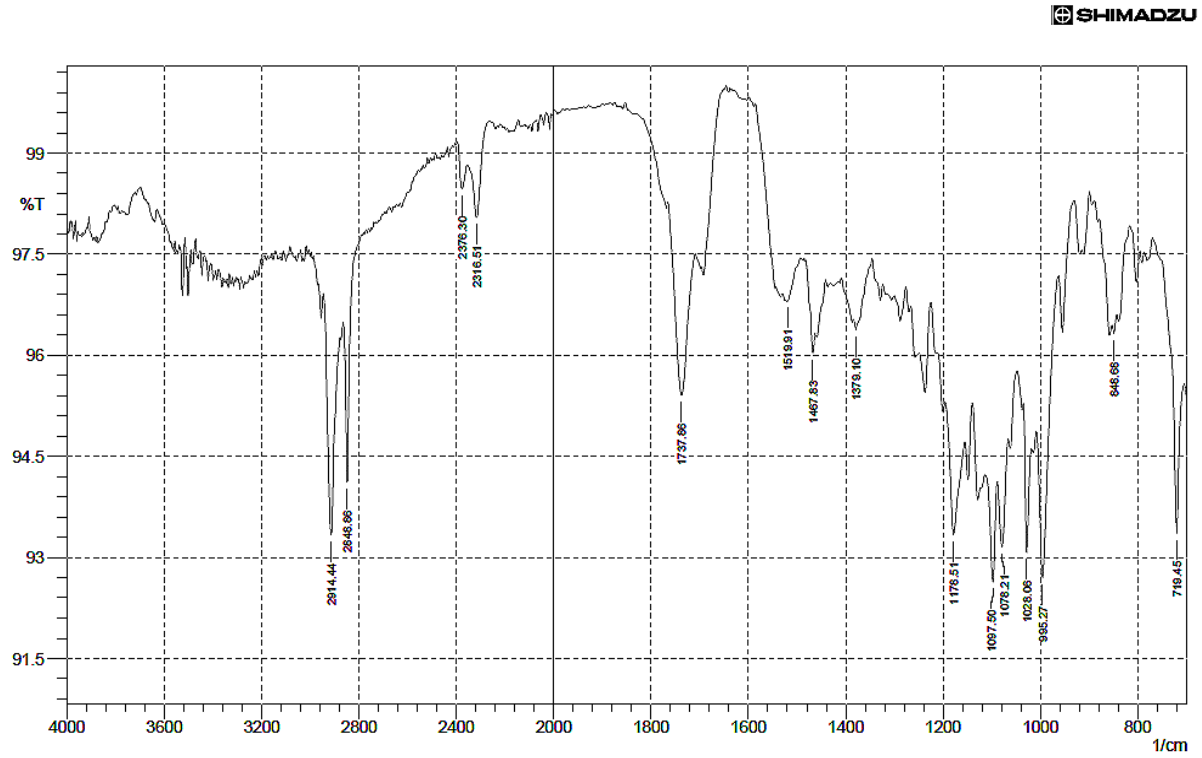

Figure 5.18 FT-IR spectrum of placebo solid lipid nanoparticles

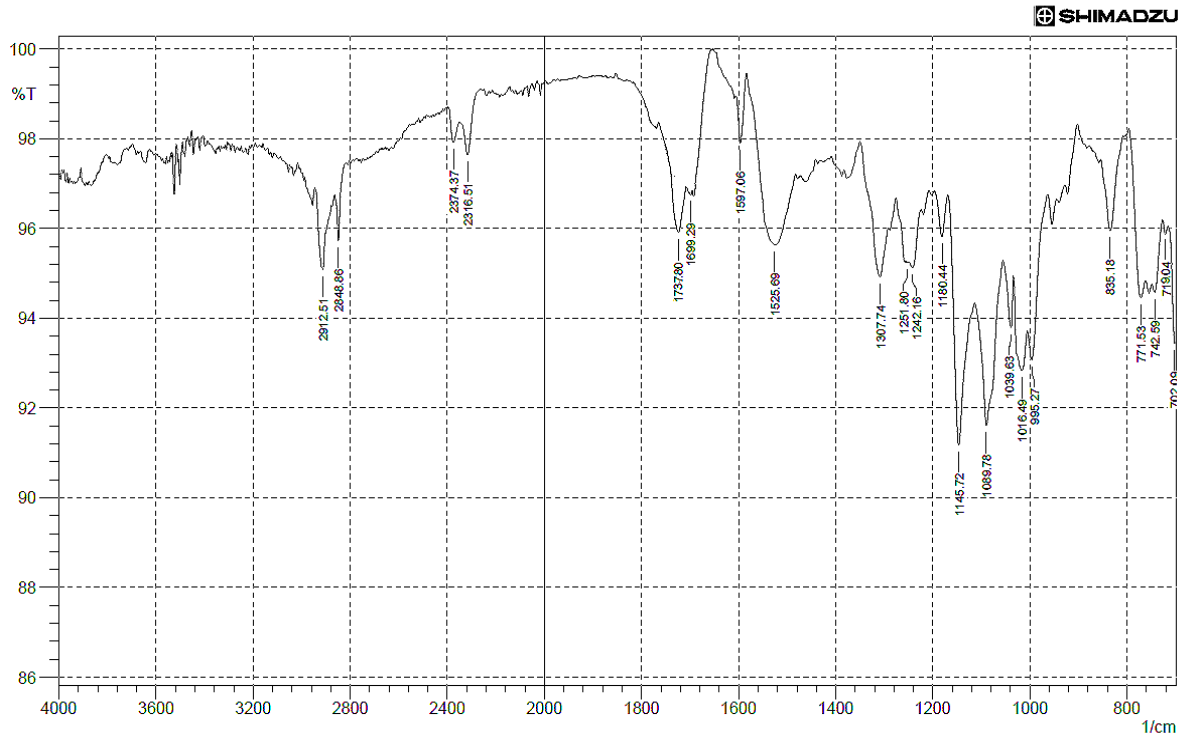

Figure 5.19 FT-IR spectrum of Darunavir loaded SLNs (Dar-SLN02)

Table 5.3 Characteristic peaks of Darunavir observed in various samples

Sample	**NH bending, primary amine**	**CO stretching (epoxy/oxirane rings)**	**CN stretching, tertiary amine**	**Aryl thio stretching**	**C-O-C stretching**
Normal range	1650-1590 cm^{-1}	1300-1200 cm^{-1}	1210-1150 cm^{-1}	715-670 cm^{-1}	1150-1010 cm^{-1}
Drug spectrum	1593.20 cm^{-1}	1249.87 cm^{-1}	1180.52 cm^{-1}	700.16 cm^{-1}	1145.01 cm^{-1}
Physical mixture spectrum	1595.13 cm^{-1}	1251.59 cm^{-1}	1180.44 cm^{-1}	702.09 cm^{-1}	1145.72 cm^{-1}
Lyophilized formulation	1597.06 cm^{-1}	1251.80 cm^{-1}	1180.44 cm^{-1}	702.09 cm^{-1}	1145.72 cm^{-1}

Table 5.4 Characteristics FT-IR peaks of lipid observed in various samples

Sample	**CH_2 stretching (cm^{-1})**	**-C=O stretching (cm^{-1})**	**Methylene $(CH_2)_n$ rocking (n>= 3) (cm^{-1})**
Normal range	2935-2910, 2865-2845	1760-1680	750-720
Lipid spectrum	2914.44, 2846.33	1737.86	719.45
Placebo SLNs	2914.44, 2846.86	1737.86	719.45
Physical mixture spectrum	2914.44, 2846.86	1737.86	719.59
Lyophilized formulation	2912.51, 2848.86	1737.80	719.04

5.7.1.6 *In-vitro* drug release of Darunavir loaded SLNs

In-vitro drug release studies for Darunavir loaded nanoparticles and plain drug suspension are shown in Table 5.5 and Figure 5.20. The plain drug suspension released 8.9 % of drug in the initial 2 hr where as the nanoparticles formulations released only up to 5 %. The release of Darunavir from nanoparticles was sustained and after the change of media to intestinal fluid, the release rate from nanoparticles increased and there was about 17 % release in 12 hr indicating a good integrity of hydrogenated castor oil based SLNs of Darunavir in the release media. There was no significant difference between the release data of all the three nanoparticles ($P>0.05$) suggesting that size of nanoparticles did not significantly affect the release of drug from the system. The mucoadhesive properties of nanoparticles are reported to increase bioavailability and reduce or minimize erratic absorption (21). Moreover, absorption of nanoparticles occurs through mucosa of the intestine by several mechanisms, namely through peyer's patches, by intracellular uptake or by paracellular pathway (22). These parameters along with SLNs' adhesive property largely influence the SLNs fate *in-vivo* and also increase the SLNs uptake through intestinal membrane. Apart from SLNs uptake, lipid lysis also occur intracellulary and these results in drug release different from that obtained through *in-vitro* results. Hence, the *in-vitro* study was performed only up to 12 hr.

Table 5.5 *In-vitro* drug release profile of plain Darunavir suspension and Darunavir loaded nanoparticles

Time (h)	% drug release ± SD			
	Plain drug suspension	Dar-SLN1	Dar-SLN2	Dar-SLN3
1	4.27 ± 1.19	3.06 ± 1.18	3.95 ± 1.21	3.90 ± 1.50
2	8.93 ± 2.38	4.49 ± 2.37	4.44 ± 1.28	5.24 ± 1.54
4	11.28 ± 2.24	6.83 ± 2.23	6.19 ± 2.23	6.21 ± 2.11
8	11.50 ± 3.27	9.48 ± 3.45	10.22 ± 3.23	8.45 ± 2.35
12	-	17.37 ± 3.47	16.47 ± 3.24	14.49 ± 3.56

*Values are represented as mean ± SD, n=3

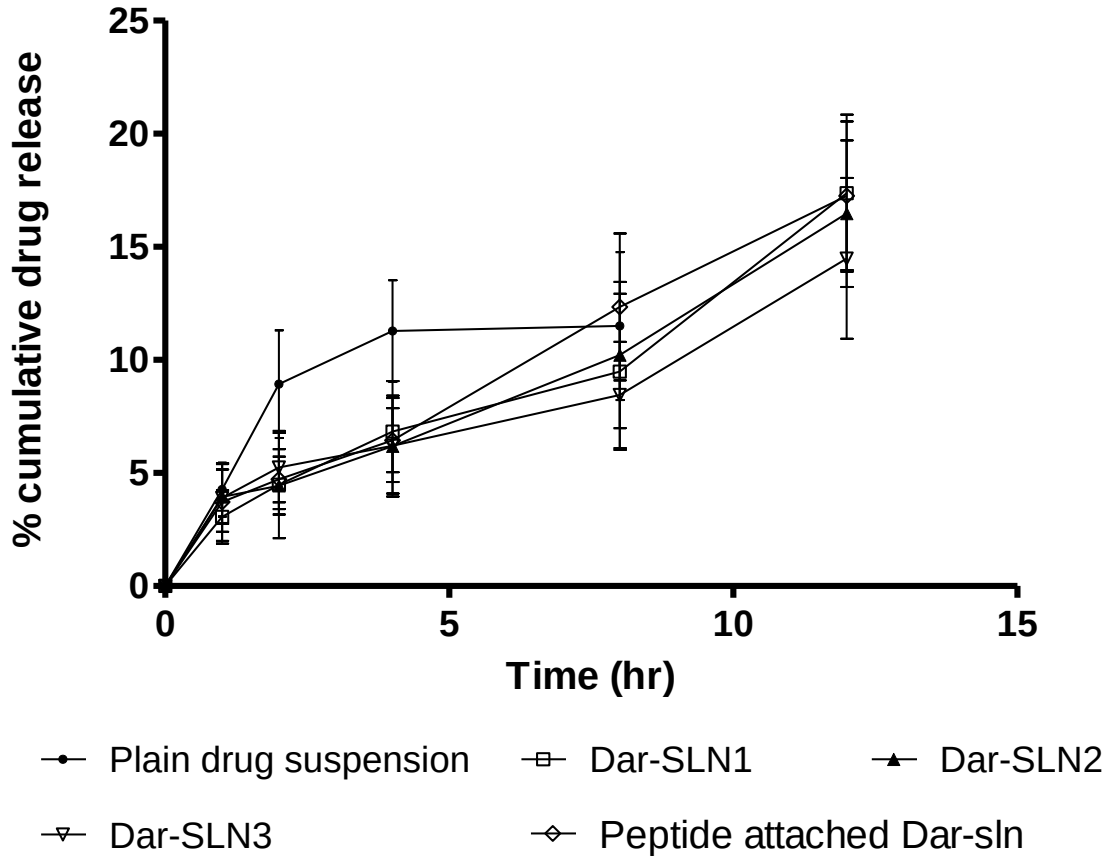

Figure 5.20 *In-vitro* drug release profiles of plain Darunavir suspension and Darunavir loaded nanoparticles

5.7.2 Characterization of peptide attached solid lipid nanoparticles of Darunavir

5.7.2.1 Particle size and zeta potential

The particle size of Pept-Dar-SLN was found to be 195.11 ± 1.53 nm with PDI 0.211 ± 0.03. The zeta potential of the formulation was obtained to be -35.45 ± 1.10 mV. There was an insignificant increase in particle size (from 189 nm to 195 nm) and a significant increase in zeta potential (from -50.1 mV to -35.45mV) after attachment of ligand which might be due to ligand attachment on SLNs surface. The particle size after lyophilization was found to be 198 ± 2.11 nm.

5.7.2.2 Qualitative determination of bound peptide

SDS-PAGE study was used to verify the presence of peptide on nanoparticle. Dithiothreitol (DTT) was used to break the sulphate bond present in the peptide. In absence of DTT (Figure 5.21a- Non-reducing PAGE), standard peptide solution gave sharp band while no band was seen with formulation sample. On treatment with DTT (Figure 5.21b- Reducing PAGE), there was breakage of sulfate band and sharp band was seen in the formulation samples. These bands were similar to that of the standard peptide band thus confirming the attachment of peptide on SLNs surface.

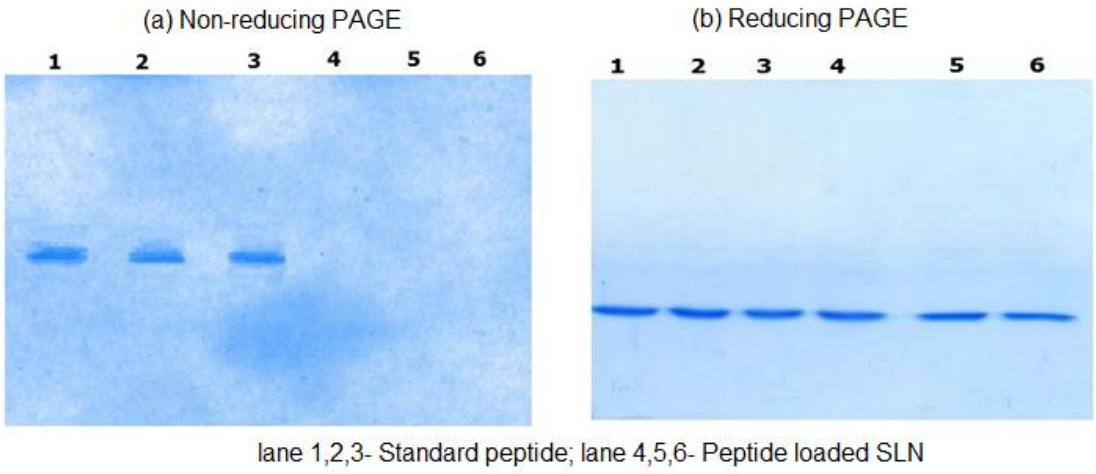

Figure 5.21 SDS Page images. Lane 1,2,3 = Peptide (standard), Lane 3,4,5 = Formulation (quantity equivalent to standard peptide)

5.7.2.3 Quantitative determination of bound peptide

The calibration plot of BSA was prepared in order to estimate the amount of peptide attached to SLN. The absorbances obtained at different BSA concentrations are given in Table 5.6. The calibration plot is shown in Figure 5.22. From the readings, the % conjugation was calculated to be 73.12 % (Table 5.7).

Table 5.6 Calibration plot of BSA

BSA Concentration (µg/ml)	Absorbance (mean ± SD)
10	0.171 ± 0.009

20	0.215 ± 0.008
30	0.249 ± 0.01
40	0.292 ± 0.007
50	0.331 ± 0.06

* n=3

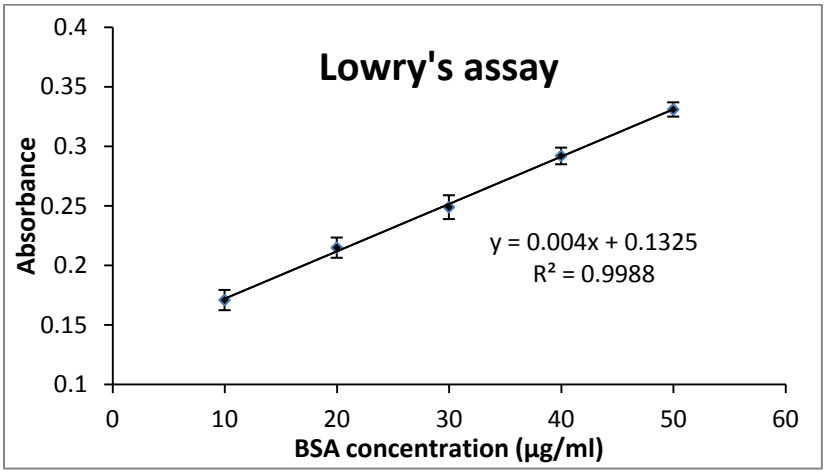

Figure 5.22 Calibration plot of BSA

Table 5.7 Results of quantitative estimation of bound peptide in Pept-Dar-SLN formulation

Absorbance of sample	Concentration of sample (µg/ml)	Dilution factor	Practical amount of peptide in 0.5ml of Pept-Dar-SLN	Theoretical amount of peptide in 0.5 ml sample	% conjugation
0.245 ±0.003	28.125 µg/ml	10	365.62 µg	500 µg	73.12 %

5.7.2.4 *In-vitro* drug release study

There was no significant difference between the release data for peptide grafted and peptide non-grafted (P>0.05) SLNs of Darunavir. These date suggested that the

grafting of peptide gave no significant effect on the release of drug from the nanoparticles. However, effect of *in-vitro* release conditions on stability of peptide was difficult to predict in this study as this would require the covalent breakage of bond between peptide and lipid and then do the quantitative estimation of the peptide to ensure its stability. Extensive literature search was done but no such study was reported.

Table 5.8 *In-vitro* drug release profile of peptide grafted Darunavir SLNs (Pept-Dar-SLN) in comparison to non-peptide grafted Darunavir SLNs (Dar-SLN2)

Time (hr)	% drug release	
	Dar-SLN2	Pept-Dar-SLN
1	3.95 ± 1.21	3.72 ± 1.72
2	4.44 ± 1.28	4.73 ± 1.32
4	6.19 ± 2.23	6.45 ± 1.42
8	10.22 ± 3.23	12.34 ± 3.25
12	16.47 ± 3.24	17.26 ± 3.28

*Values are represented as mean ± SD, n=3

5.7.3 Characterization of nanoemulsion of Darunavir

5.7.3.1 Globule size, PDI and zeta potential

The globule size, PDI and zeta potential of formulated nanoemulsion of Darunavir were found to be 209.5 ± 2.36 nm, 0.150 ± 0.03 and -41.1 ± 1.46 mV respectively. The low PDI value indicates more uniformity in the globule sizes.

5.7.3.2 Electrical conductivity

The electrical conductivity of DNE-3 was found to be 2.94 ± 0.05 mS/cm.

5.7.3.3 Drug loading

The drug loading of DNE-3 formulation was found to be 7.63 ± 0.09 mg/ml.

5.7.3.4 Transmission electron microscopy

Figure 5.23 shows TEM image of optimized nanoemulsion DNE-3 of Darunavir. The image revealed the discrete and round structures without aggregation.

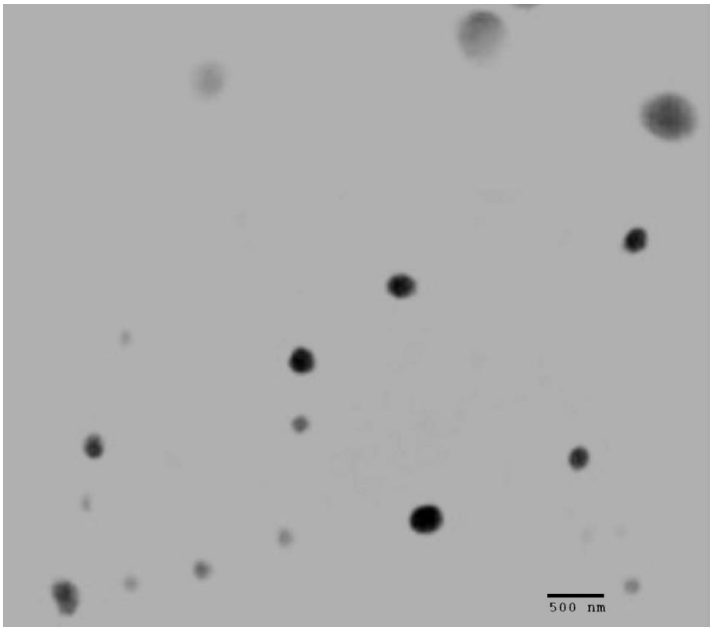

Figure 5.23 Transmission electron microscopic image of DNE-3 formulation

5.7.3.5 *In-vitro* drug release study

***In-vitro* drug release studies of optimized batch of Darunavir loaded nanoemulsion (DNE3) in comparison with plain drug suspension is shown in**

Table 5.9 and Figure 5.24. In comparison to plain drug suspension, higher release was obtained with nanoemulsion indicating higher solubilization of drug due to presence of lipid. The release of Darunavir from nanoemulsion was sustained and took 12 hr to release 95% of drug. The results of the kinetic model fitting are shown in

Table 5.10. Highest R^2 value was obtained with Higuchi model indicating that the drug release mechanism was the lipid matrix diffusion based on Fick's law (1). The Higuchi plot of cumulative % drug released Vs root of time is shown in Figure 5.25.

Table 5.9 *In-vitro* drug release of Darunavir loaded nanoemulsion (DNE3) in comparison with plain Darunavir suspension

Time (hr)	% drug release ± SD	
	Plain drug suspension	Optimized Darunavir loaded nanoemulsion (DNE3)
1	4.27 ± 1.19	20.27 ± 2.34
2	8.93 ± 2.38	33.16 ± 2.52
4	11.28 ± 2.24	55.17 ± 5.26
8	11.50 ± 3.27	76.27 ± 4.25
12	-	95.32 ± 4.75

*Values are represented as mean ± SD, n=3

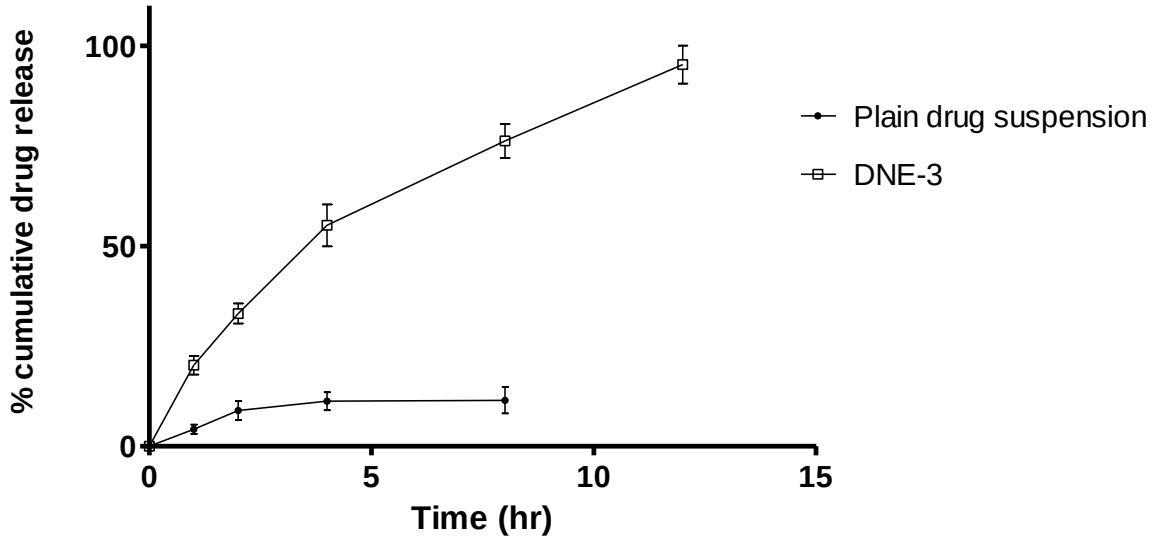

Figure 5.24 *In-vitro* drug release profiles of Darunavir loaded nanoemulsion (DNE3) in comparison with plain Darunavir suspension

Table 5.10 Release kinetics of optimized Darunavir loaded nanoemulsion (DNE3) formulation

Formulation	R^2 value				
	Zero order	**First order**	**Higuchi model**	**Hixon-crowell model**	**Korsmeyer-peppas model**
DNE 03	0.9618	0.8506	**0.9960**	0.9896	0.9917

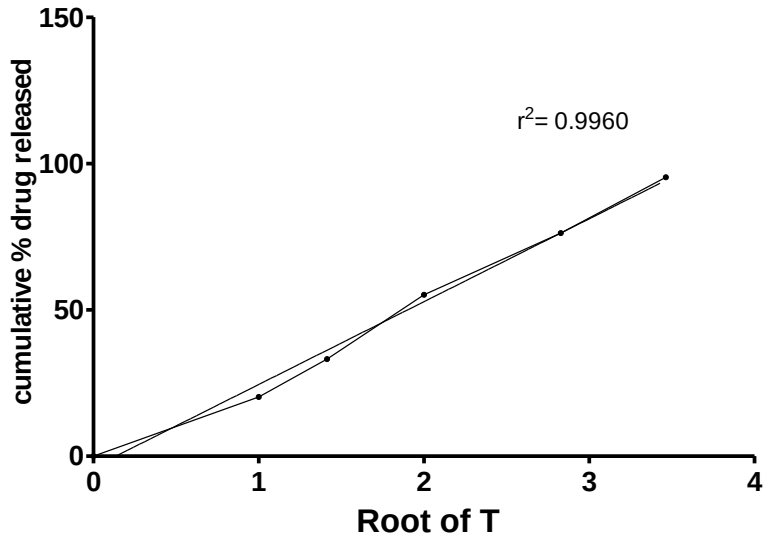

Figure 5.25 Plot of cumulative % drug release from DNE-3 versus root of time

Kinetics as well as prolonged drug release observed can be explained by the fact that Darunavir diffusion from the oily core and interface is hindered by the aqueous medium, which acts as a barrier to drug transport due to its low solubility in water. Such sustained drug delivery from nanoemulsion is frequently reported in the literature (23, 24) and may occur *in-vivo*. It is worth mentioning that the dialysis membrane also accomplishes a physical separation of the nanoemulsions from the Darunavir released to the medium and may be in part responsible for this feature. This technique is criticized by some authors for not mimicking *in-vivo* conditions and release mechanism.

5.7.4 Characterization of optimized ATZ loaded solid lipid nanoparticles (ALN-23) and peptide grafted ATZ loaded SLNs (Pept-ATZ-SLN)

5.7.4.1 Particle size and zeta potential

Figure 5.26 shows the particle size distribution of ALN-23 formulation. The mean particle size was found to be 190.1 ± 2.45 nm along with PDI of 0.153 ± 0.06. The zeta potential distribution is shown in Figure 5.27. The mean zeta potential was obtained as -42.63 ± 2.46 mV. The particle size of Pept-ATZ-SLN was found to be 194.65 ± 1.15 nm with PDI 0.104 ± 0.03. The zeta potential of the formulation was obtained to be -33.64 ± 2.17 mV. There was an insignificant increase in particle size (from 190 nm to 194 nm) and a significant increase in zeta potential (from -42.63 mV to -33.64 mV) after attachment of ligand which might be due to ligand attachment on SLNs surface.

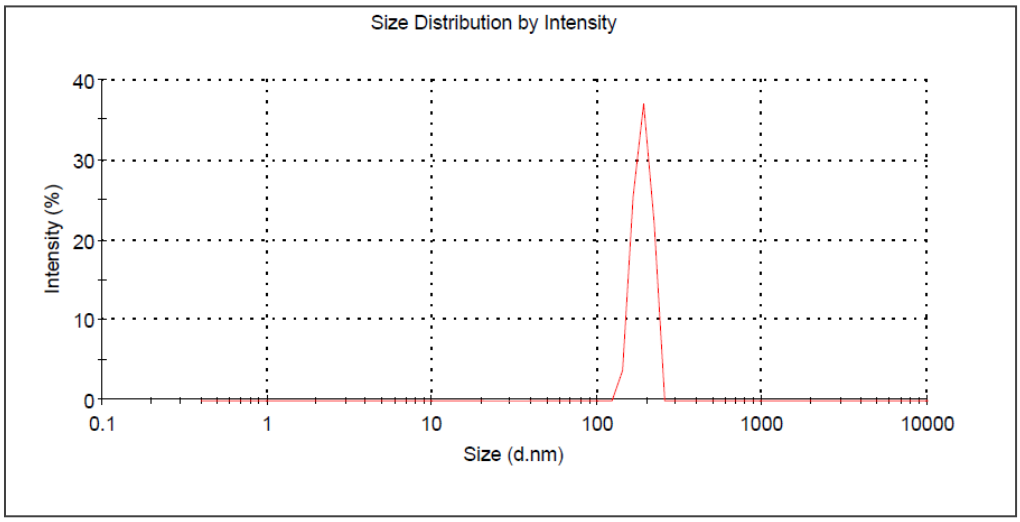

Figure 5.26 Particle size distribution of ALN-23 formulation by Malvern Zetasizer

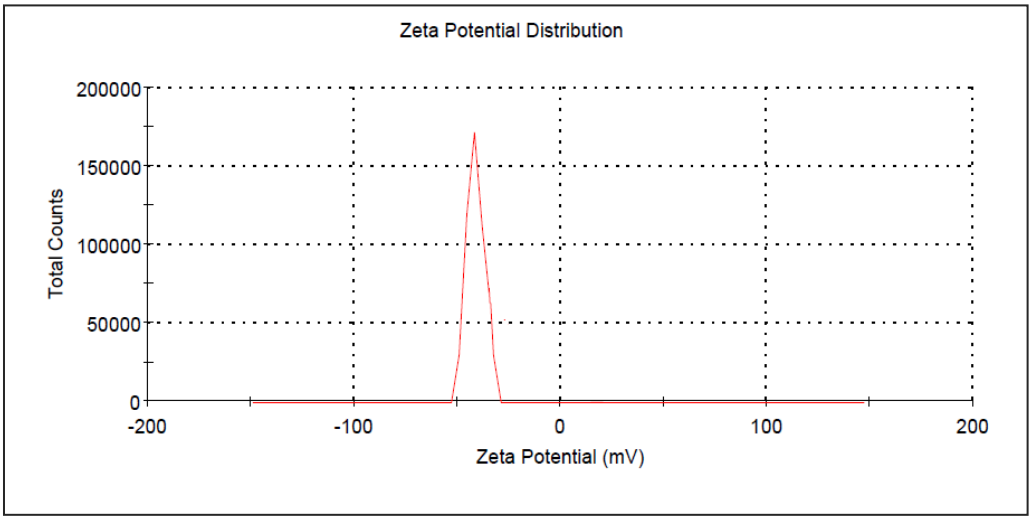

Figure 5.27 Zeta potential distribution of ALN-23 formulation by Malvern Zetasizer

5.7.4.2 Entrapment efficiency (EE) and drug loading

The EE for optimized ATZ loaded SLNs was found to be 94.26 ± 2.12 % and its drug loading was estimated to be 8.00 ± 0.4 % w/w.

5.7.4.3 Transmission electron microscopy (TEM) and Field emission scanning electron microscopy (FE-SEM)

Figure 5.28 and Figure 5.29 shows transmission electron microscopic and Field emission scanning electron microscopic images of optimized ATZ loaded nanoparticles respectively. The images revealed the discrete and round structures without aggregation and the diameter of nanoparticles formulation was in accordance with the results obtained through size analysis (Malvern zetasizer).

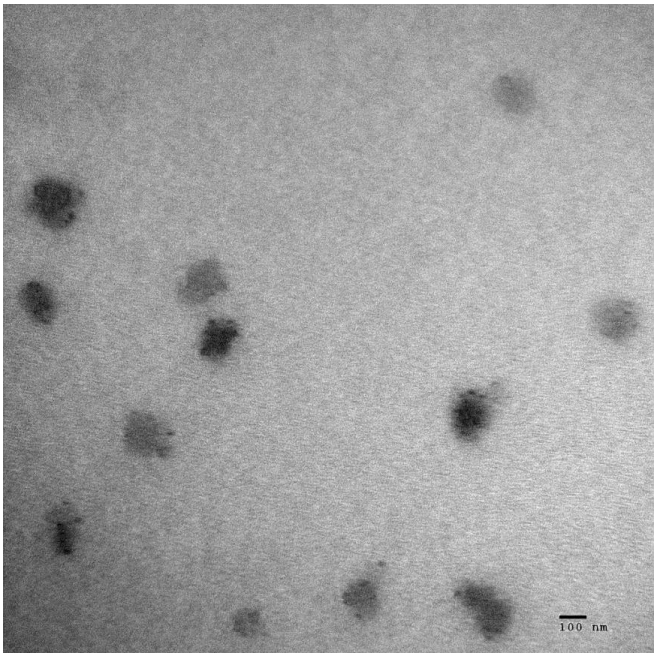

Figure 5.28 Transmission electron microscopic image of ALN-23 formulation

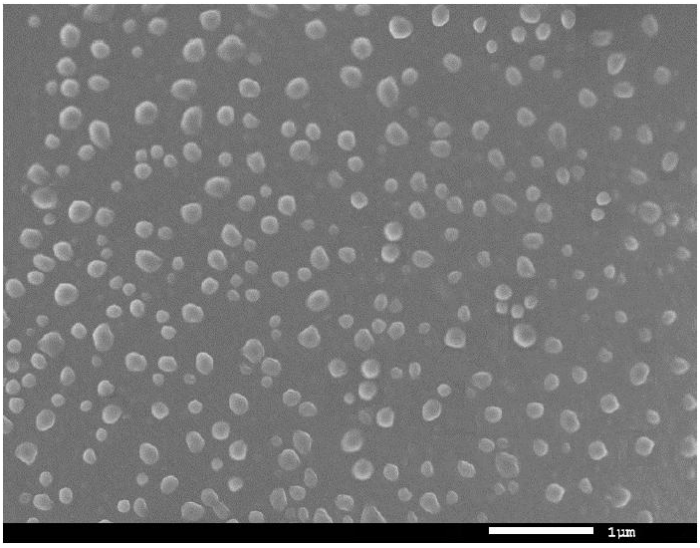

Figure 5.29 Field emission scanning electron microscopic image of ALN-23 formulation

5.7.4.4 Differential scanning calorimetric (DSC) studies

For assessment of miscibility of drug in lipid matrices, DSC study was done. The DSC thermogram of pure drug showed a sharp endothermic peak at 198.79ºC corresponding to its melting point (Figure 5.30a). DSC thermogram of lipid showed two

endothermic peaks at 75.93ºC and 84.17ºC due to its two isoforms. Absence of drug peak in the DSC thermograms of physical mixture and lyophilized nanoparticles shows that drug got solubilized in the lipid matrices completely.

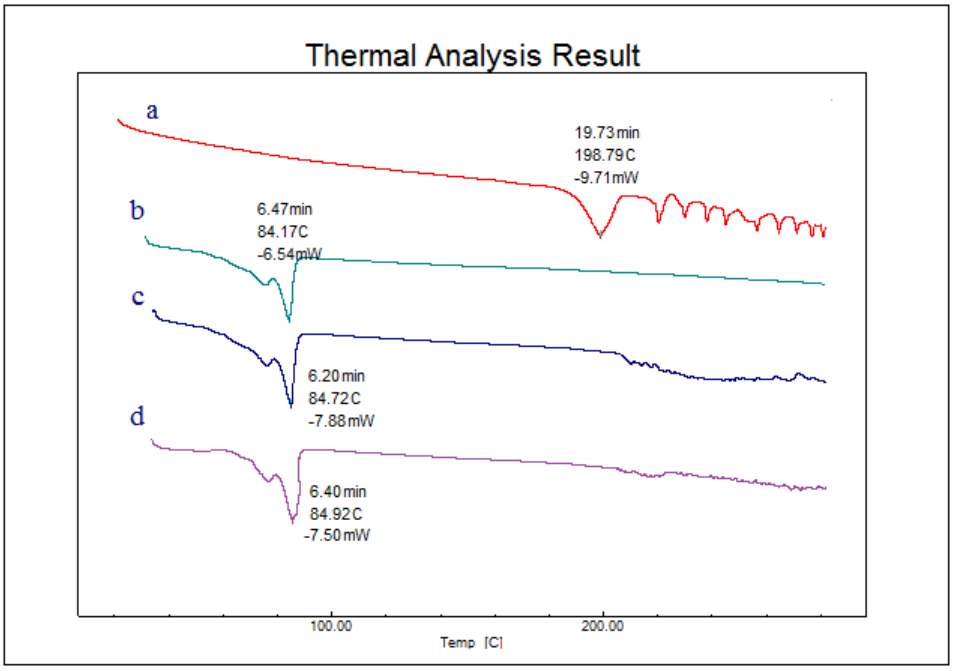

Figure 5.30 Overlay plot of DSC thermograms of (a) pure ATZ, (b) lipid, (c) physical mixture of drug and lipid and (d) lyophilized ATZ loaded SLNs

5.7.4.5 Fourier transform infrared (FT-IR) spectroscopy

FT-IR spectrum of pure drug (Figure 5.31) showed characteristic peaks of –C=O stretching at 1697.36 cm^{-1}, aliphatic secondary amine stretching at 3312.40 cm^{-1}, secondary amine stretching bending at 1550.77 cm^{-1} and C-N stretching at 1240 and 1271 cm^{-1} (19, 20). HCO showed characteristic peaks as mentioned in section 5.7.1.5. The spectrum of physical mixture (Figure 5.32) and lyophilized formulation (Figure 5.33) showed characteristic peaks of both drug and lipid as shown in Table 5.11 and Table 5.12 indicating compatibility of drug with excipients.

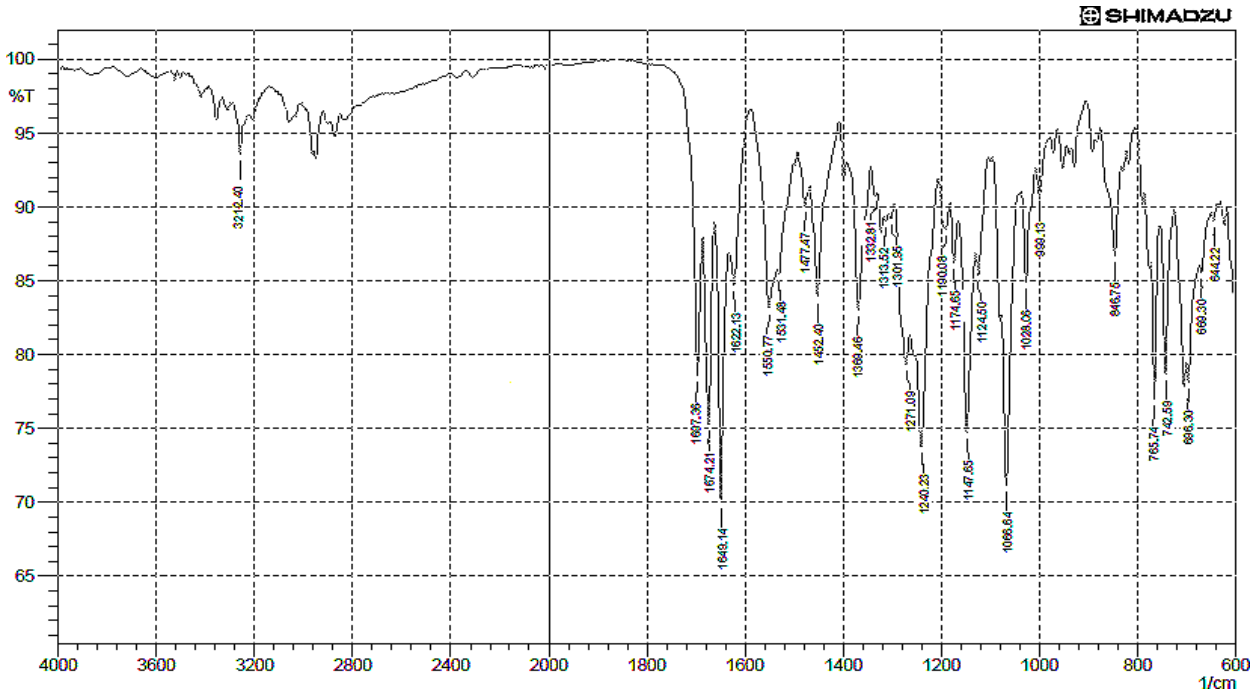

Figure 5.31 FT-IR spectrum of Atazanavir sulfate

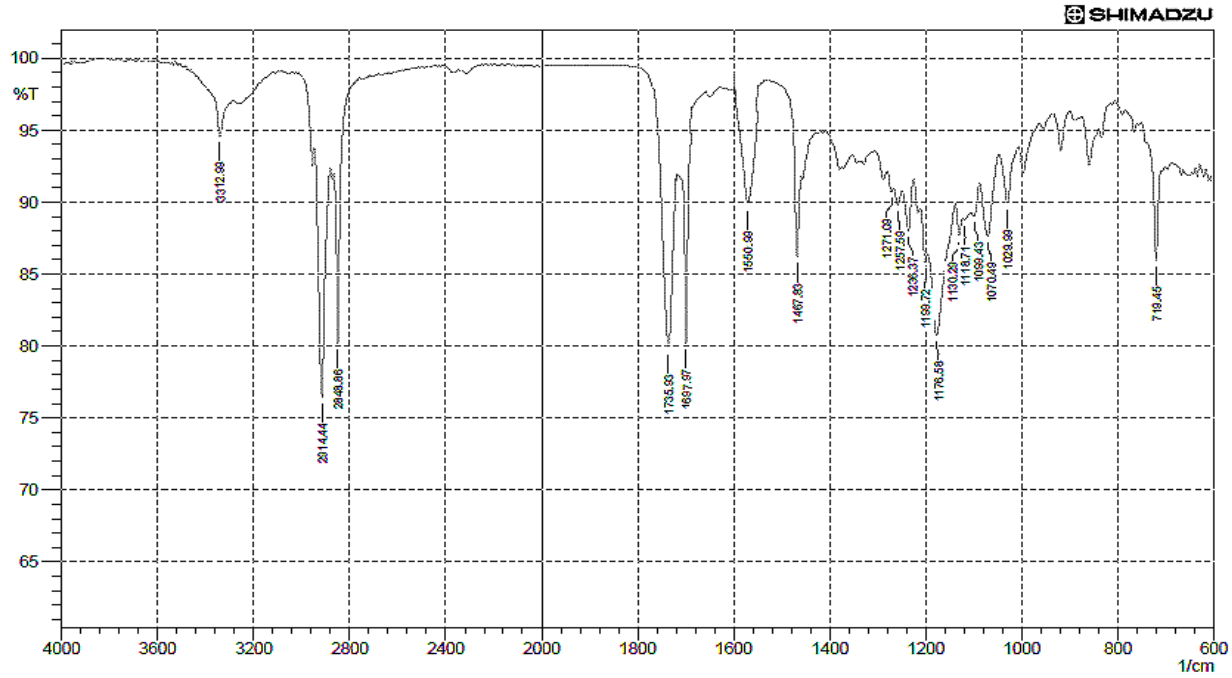

Figure 5.32 FT-IR specctrum of physical mixture of ATZ and HCO

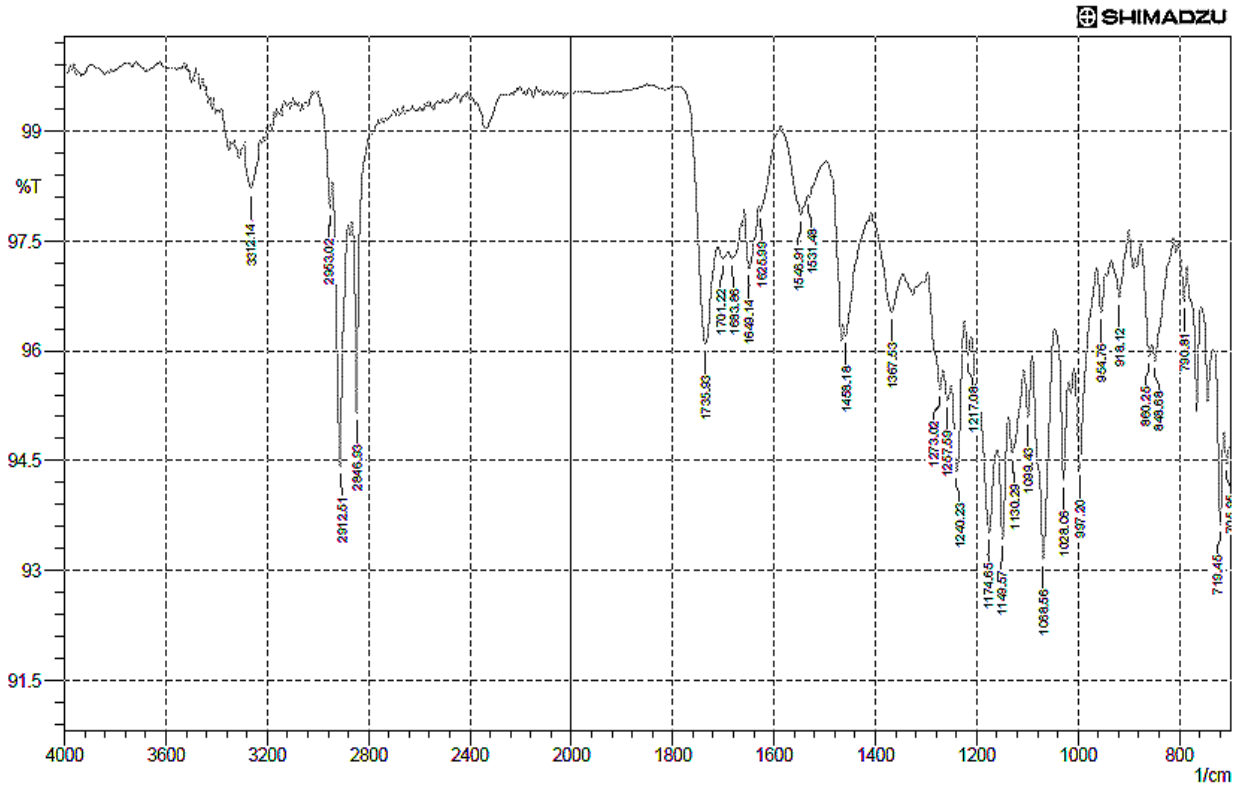

Figure 5.33 FT-IR spectrum of lyophilized formulation ALN-23

Table 5.11 Characteristic peaks of ATZ observed in various samples

Sample	**Aliphatic 2º amine stretching (cm^{-1})**	**-C=O stretching (cm^{-1})**	**Secondary amine bending (cm^{-1})**	**-C-N stretching (cm^{-1})**
Normal range	3360-3310	1680-1760	1650-1550	1360-1180
Drug spectrum	3312.40	1697.36	1550.77	1271.09, 1240.23
Physical mixture spectrum	3312.99	1697.97	1550.99	1271.09 1236.37
Lyophilized formulation	3312.14	1698.86	1546.91	1240.23, 1273.02

Table 5.12 Characteristics peaks of lipid observed in various samples

Sample	**CH_2 stretching (cm^{-1})**	**-C=O stretching (cm^{-1})**	**Methylene $(CH_2)_n$ rocking (n>= 3) (cm^{-1})**
Normal range	2935-2910, 2865-2845	1760-1680	750-720
Lipid spectrum	2914.44, 2846.33	1737.86	719.45
Physical mixture spectrum	2914.44, 2846.86	1735.93	719.45
Lyophilized formulation	2912.51, 2846.33	1735.93	719.45

5.7.4.6 Qualitative determination of surface grafted peptide

SDS-PAGE study was used to confirm the presence of peptide on nanoparticle. Dithiothreitol (DTT) was used to break the sulphate bond present in the peptide. In absence of DTT (Figure 5.34a- Non-reducing PAGE), standard peptide solution gave sharp band while no bands were seen with formulation samples. On treatment with DTT (Figure 5.34b- Reducing PAGE), there was breakage of sulfate band and sharp bands were seen in the formulation samples. These bands were similar to that of the standard peptide bands thus confirming the attachment of peptide on SLNs surface.

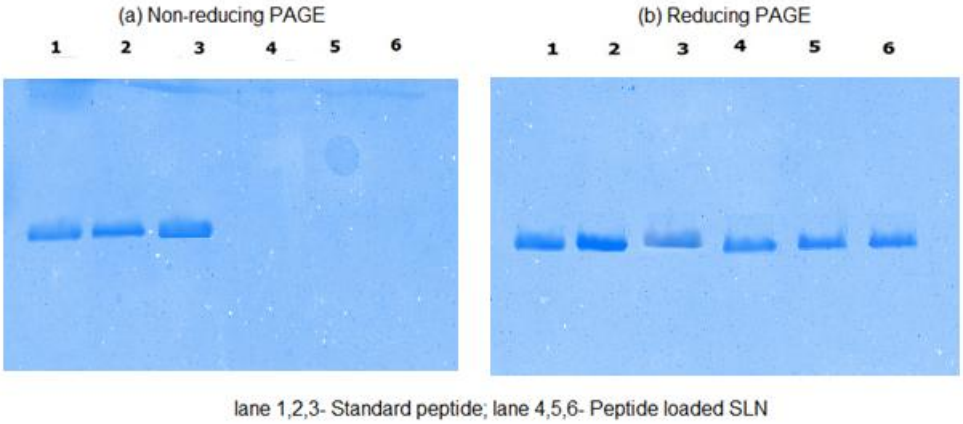

Figure 5.34 SDS Page images. Lane 1,2,3 = Peptide (standard), Lane 3,4,5 = Formulation (quantity equivalent to standard peptide)

5.7.4.7 Quantitative determination of surface grafted peptide

The calibration curve of BSA plotted is given in section 5.7.2.3. The absorbance of peptide loaded formulation is given Table 5.13 and from the reading, % conjugation of peptide to the nanoparticles was calculated to be 76.37 %.

Table 5.13 Results of quantitative estimation of bound peptide in Pept-ATZ-SLN formulation

Mean absorbance of sample	Concentration of sample (µg/ml)	Dilution factor	Practical amount of peptide in 0.5ml of Pept-Dar-SLN	Theoretical amount of peptide in 0.5 ml sample	% conjugation
0.250±0.002	29.375 µg/ml	10	381.875 µg	500 µg	76.37 %

*n=3

5.7.4.8 *In-vitro* drug release of Atazanavir loaded solid lipid nanoparticles

In-vitro drug release studies for ATZ loaded nanoparticles and plain drug suspension is shown in Table 5.14 and Figure 5.35. Only 10 % of drug released from plain suspension in first 2 hr in SGF. After changing media to SIF, the release rate decreased and in 8 hr only 13% of drug was released. In case of nanoparticles, the release was found to be sustained and only 4.26 % drug was released in first 2 hr in gastric medium. After the change of media to intestinal fluid, the release rate from nanoparticles increased and there was about 20 % release in 12 hr. There was insignificant change in ATZ release upon peptide grafting on SLNs indicating that peptide grafting on SLNs surface gave no effect on ATZ release.

Table 5.14 *In-vitro* drug release profile of plain ATZ suspension and ATZ loaded nanoparticles

Time (hr)	% drug release ± SD		
	Plain drug suspension	Optimized ATZ loaded lipid SLNs (ALN-23)	Peptide grafted ATZ loaded SLNs (Pept-ATZ-SLNs)
1	6.38 ± 2.18	2.75 ± 1.32	3.10 ± 1.16
2	10.45 ± 2.37	4.26 ± 2.65	5.38 ± 2.17
4	12.27 ± 3.27	8.24 ± 2.75	9.84 ± 3.11
8	13.78 ± 4.28	13.93 ± 3.20	14.87 ± 3.82
12	-	20.25 ± 4.27	21.13 ± 4.24

*Values are represented as mean ± SD, n=3

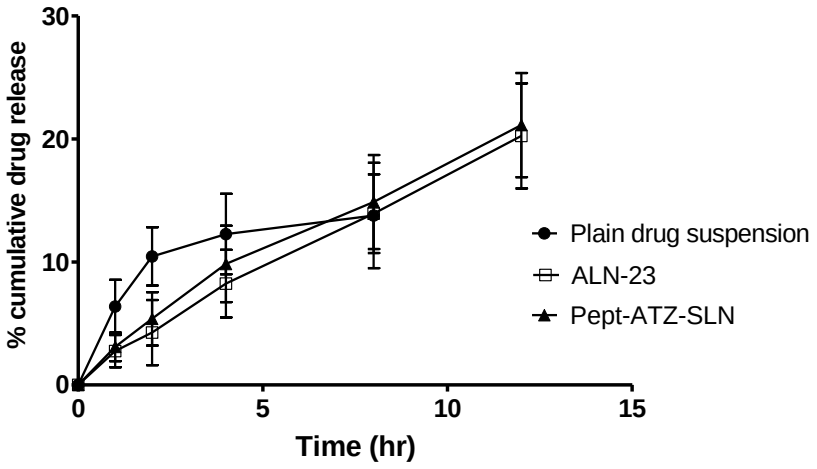

Figure 5.35 *In-vitro* drug release profiles of plain ATZ suspension and ATZ loaded nanoparticles

5.8 References

1. Costa P, Lobo JMS. Modeling and comparison of dissolution profiles. European journal of pharmaceutical sciences. 2001;13(2):123-33.
2. Higuchi T. Rate of release of medicaments from ointment bases containing drugs in suspension. Journal of pharmaceutical sciences. 1961 Oct;50:874-5.

3. Higuchi T. Mechanism of Sustained-Action Medication. Theoretical Analysis of Rate of Release of Solid Drugs Dispersed in Solid Matrices. Journal of pharmaceutical sciences. 1963 Dec;52:1145-9.
4. Korsmeyer RW, Gurny R, Doelker E, Buri P, Peppas NA. Mechanisms of potassium chloride release from compressed, hydrophilic, polymeric matrices: effect of entrapped air. Journal of pharmaceutical sciences. 1983 Oct;72(10):1189-91.
5. Peppas NA. Analysis of Fickian and non-Fickian drug release from polymers. Pharmaceutica acta Helvetiae. 1985;60(4):110-1.
6. Hixson A, Crowell J. Dependence of reaction velocity upon surface and agitation. Industrial & Engineering Chemistry. 1931;23(10):1160-8.
7. Jain A, Agarwal A, Majumder S, Lariya N, Khaya A, Agrawal H, et al. Mannosylated solid lipid nanoparticles as vectors for site-specific delivery of an anti-cancer drug. Journal of Controlled Release. 2010;148(3):359-67.
8. Preparation note. Dialysis tubing cellulose membrane. Sigma-aldrich. http://www.sigmaaldrich.com/catalog/product/sigma/d9652?lang=en&region=IN. Accessed March, 2012.
9. Kawakami K, Yoshikawa T, Hayashi T, Nishihara Y, Masuda K. Microemulsion formulation for enhanced absorption of poorly soluble drugs: II. In vivo study. Journal of controlled release. 2002;81(1):75-82.
10. Neves AR, Lucio M, Martins S, Lima JL, Reis S. Novel resveratrol nanodelivery systems based on lipid nanoparticles to enhance its oral bioavailability. International journal of nanomedicine. 2013;8:177-87.
11. Life technologies Available from: https://www.lifetechnologies.com/in/en/home/references/protocols/proteins-expression-isolation-and-analysis/sds-page-protocol.html Accessed Jan 2014.
12. Life technologies. Available from: https://tools.lifetechnologies.com/content/sfs/brochures/1601925-Electrophoresis-Handbook.pdf Accessed Jan 2014.
13. Lowry OH, Rosebrough NJ, Farr AL, Randall RJ. Protein measurement with the Folin phenol reagent. The Journal of biological chemistry. 1951 Nov;193(1):265-75.

14. Patel RB, Patel MR, Bhatt KK, Patel BG. Formulation and evaluation of microemulsion-based drug delivery system for intranasal administration of olanzapine. Int J Bimed Pharm Sci. 2013;7:20-7.
15. Patravale V, Dandekar P, Jain R. Nanoparticulate drug delivery: Perspectives on the transition from laboratory to market: Elsevier; 2012.
16. Nidhin M, Indumathy R, Sreeram K, Nair BU. Synthesis of iron oxide nanoparticles of narrow size distribution on polysaccharide templates. Bulletin of Materials Science. 2008;31(1):93-6.
17. Yang D, Hrymak AN. Crystal Morphology of hydrogenated castor oil in the crystallization of oil-in-water emulsions: Part I. Effect of temperature. Industrial & Engineering Chemistry Research. 2011;50(20):11585-93.
18. Aji Alex MR, Chacko AJ, Jose S, Souto EB. Lopinavir loaded solid lipid nanoparticles (SLN) for intestinal lymphatic targeting. European journal of pharmaceutical sciences : official journal of the European Federation for Pharmaceutical Sciences. 2011;42(1-2):11-8.
19. Coates J. Interpretation of Infrared spectra, A practical approach. In: Meyers RA, editor. Encyclopedia of Analytical chemistry. Chichester: John Wiley & sons Ltd; 2000. p. 10815-37.
20. Chatwal G, Anand S. Instrumental Methods of Chemical Analysis-Gurdeep Chatwal, pp2. 389-2.398. Himalaya publishing house pvt. ltd.
21. Ponchel G, Montisci M-J, Dembri A, Durrer C, Duchêne D. Mucoadhesion of colloidal particulate systems in the gastro-intestinal tract. Eur J Pharm Biopharm. 1997;44(1):25-31.
22. Üner M, Yener G. Importance of solid lipid nanoparticles (SLN) in various administration routes and future perspectives. International journal of nanomedicine. 2007;2(3):289.
23. Chavhan SS, Petkar KC, Sawant KK. Simvastatin nanoemulsion for improved oral delivery: design, characterisation, in vitro and in vivo studies. Journal of microencapsulation. 2013;30(8):771-9.

24. Kelmann RG, Kuminek G, Teixeira HF, Koester LS. Carbamazepine parenteral nanoemulsions prepared by spontaneous emulsification process. International journal of pharmaceutics. 2007;342(1):231-9.